

Coordinates

Volume XVIII, Issue 6, June 2022

THE MONTHLY MAGAZINE ON POSITIONING, NAVIGATION AND BEYOND

Spatial analysis of soil

trace element contaminants
in Urban public open space

Scientific project for monitoring of geodynamic processes in Sofia



0.05°
ATTITUDE

0.02°
HEADING

1 cm
POSITION

NEW ELLIPSE-D

The Smallest Dual Frequency & Dual Antenna INS/GNSS

- » RTK Centimetric Position
- » Quad Constellations
- » Post-processing Software



Ellipse-D
RTK Dual Antenna



Ellipse-N
RTK Single Antenna



OEM
RTK Best-in-class SWaP-C



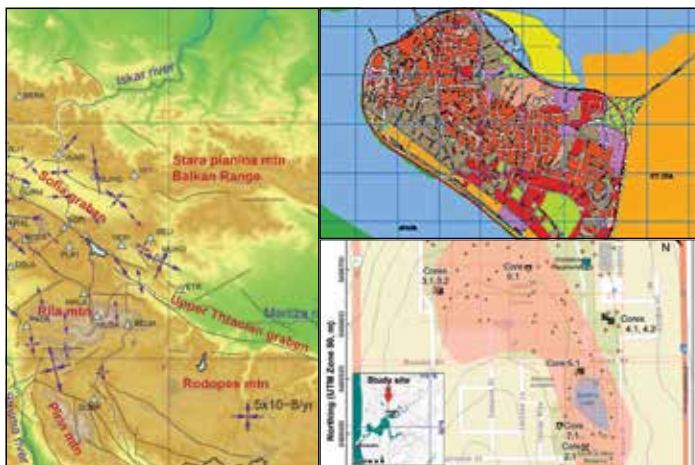
ION GNSS+ 2022

September 19-23, 2022

Show Dates: September 21 and 22

Hyatt Regency Denver at Colorado Convention Center
Denver, Colorado

REGISTER TODAY
[ION.ORG/GNSS](https://ion.org/gnss)



In this issue

Coordinates Volume 18, Issue 6, June 2022

Articles

- Scientific project for monitoring of geodynamic processes in Sofia** NIKOLAY DIMITROV 6 **Spatial analysis of soil trace element contaminants in urban public open space** ANDREW W RATE 11 **Mapping physical development changes using Geospatial techniques** LEONARD MICHAEL ONYINYECHE AMINIGBO 24

Columns

- My Coordinates** EDITORIAL 5 **Old Coordinates** 31 **News** GEODESY 9 GIS 32 GNSS 33 IMAGING 34 LBS 35 UAV 36
INDUSTRY 36 **Mark Your Calendar** 38

This issue has been made possible by the support and good wishes of the following individuals and companies
Andrew W Rate, Leonard Michael Onyinyechi Aminigbo and Nikolay Dimitrov; Labsat, SBG System, and many others.

Mailing Address

A 002, Mansara Apartments
C 9, Vasundhara Enclave
Delhi 110 096, India.
Phones +91 11 42153861, 98102 33422, 98107 24567

Email

[information] talktous@mycoordinates.org
[editorial] bal@mycoordinates.org
[advertising] sam@mycoordinates.org
[subscriptions] iwant@mycoordinates.org
Web www.mycoordinates.org

Coordinates is an initiative of CMPL that aims to broaden the scope of positioning, navigation and related technologies. CMPL does not necessarily subscribe to the views expressed by the authors in this magazine and may not be held liable for any losses caused directly or indirectly due to the information provided herein. © CMPL, 2022. Reprinting with permission is encouraged; contact the editor for details.

Annual subscription (12 issues)
[India] Rs.1,800 [Overseas] US\$100

Printed and published by Sanjay Malaviya on behalf of Coordinates Media Pvt Ltd

Published at A 002 Mansara Apartments, Vasundhara Enclave, Delhi 110096, India.

Printed at Thomson Press (India) Ltd, Mathura Road, Faridabad, India

Editor Bal Krishna

Owner Coordinates Media Pvt Ltd (CMPL)

This issue of Coordinates is of 40 pages, including cover.



@jacques70 | Dreamstime.com

Mapping the Moon

In 2020, it was USGS Astrogeology Science Centre
That released “Unified Geologic Map of the Moon” (1:5,000,000 scale).
Now China has released comprehensive geologic map of the moon
The most detailed one (1:2,500,000 scale).
This is the result of the efforts many Chinese scientists from several institutions,
Who have developed high-resolution topographic maps
Largely from the data gathered by China’s lunar exploration Chang’e project.
The Institute of Geochemistry of Chinese Academy of Sciences has led the project.
The map was published by Science Bulletin on 30th May 2022.
This may serve as a roadmap for planning future human missions.

Bal Krishna, Editor
bal@mycoordinates.org

ADVISORS Naser El-Sheimy PEng, CRC Professor, Department of Geomatics Engineering, The University of Calgary Canada, George Cho Professor in GIS and the Law, University of Canberra, Australia, Professor Abbas Rajabifard Director, Centre for SDI and Land Administration, University of Melbourne, Australia, Luiz Paulo Souto Fortes PhD Associate Professor, University of State of Rio Janeiro (UERJ), Brazil, John Hannah Professor, School of Surveying, University of Otago, New Zealand

Scientific project for monitoring of geodynamic processes in Sofia

The expected results will be a contribution to the assessment of natural risk and seismic hazard in the study area and will have a positive impact for the sustainable development of the region



Nikolay Dimitrov
 Assoc Professor, Head
 of Department Geodesy,
 National Institute of
 Geophysics, Geodesy
 and Geography,
 Bulgarian Academy
 of Science, Bulgaria

Introduction

The study of recent crustal movements is one of the priority areas of the Earth sciences. Geodetic methods occupy a particularly important place in the general complex of measurements and investigations of crustal movements because they provide quantitative information on the condition and development of geodynamic processes. The area of interest of this study is bounded to the north of the southern slopes of the Balkan Mountains, to the south to the southern slopes of the Rila Mountains, to the west - the western border of Bulgaria and to the east - the beginning of the Upper Thracian plain. The region is of particular interest due to its high population density and high concentration of industrial facilities and resources. Possible strong earthquakes and related hazardous processes such as landslides, settlements and collapses may cause material damage and have a negative psychological effect on the population.

Neotectonic setting of the studied area

The area of Sofia is situated in Central West Bulgaria (Fig. 1). The present-day geodynamics of the area as well as the territory of South Bulgaria is defined by the neotectonic extensional processes in the South Bulgarian Extensional Region (Burchfiel et. All, 2000), part of the broad East-Mediterranean – Balkan Extensional system. The extension is in

a general N-S direction which results in tectonic structures with general trend NW-SE to E-W. These structures are clearly expressed morphologically and define the topography of the area– elevated mountains and subsided lands. In Rila Mountain is located the highest pick of the Balkan Peninsula – Mousala (2925 m). A central position in the area has the Sofia plain which from tectonic point of view represents a neotectonic graben with complicate internal structure bordered from both sides by active faults. To the south by the Vitosha fault and to the north by the Sub-Balkan fault system (Negushevo fault system). The last fault system has a crucial role for the topography of the country forming Stara Planina (The Balkan Range) and dividing the country into two sharply distinguished morphological units. This fault was accepted to limit the northern boundary of the Aegean extension (Burchfiel et. All, 2000). However, the presence of Botevgrad graben in the studied area to the north suggests that extension, even locally has occurred further to the north inside the Stara Planina Mountain (The Balkan Range). Beside Sofia graben in the area along this fault are formed some smaller graben to the east (Sarantsi, Kamartsi and Zlatitsa), part of the Sub-Balkan Graben System (Tzankov et. All, 1996). In the area of Sofia historically are known few several stronger earthquakes with suggested magnitudes 5.5 – 7.0 (Yosifov et. All, 2018). The last one of magnitude Mw 5.6 occurred on May 22th 2012 to the NW of Sofia around Pernik town (Radulov et. All, 2012) along a fault

zone suggested to be presently active based on GPS data (Kotzev et al., 2005).

Geodynamic GNSS network around Sofia and Southwestern Bulgaria

To study the modern movements of the Earth's crust during the period 1996-1997, a geodynamic network was built in the area around Sofia, covering Central Western Bulgaria. The network is designed for high-precision GNSS measurements, determination of coordinates and velocities of points, calculation of active strain in the area and long-term monitoring crustal movements. The first GNSS measurements of the Sofia Geodynamic Network were made in 1997. Full measurement of the entire network with processing and analysis of the results has so far been performed only in two epochs 1997 and 2000 (Kotzev et al., 2001a; Kotzev et al., 2006, Dimitrov et al., 2020).

GNSS measurements 2020, processing and preliminary results

At the end of 2019th, the project "Monitoring of geodynamic processes in the region of Sofia" of the Department of Geodesy, the National Institute of Geophysics, Geodesy and Geography at BAS, funded by the National Research Fund, was launched. This allowed for a new comprehensive measurement of the geodynamic network. The campaign was accomplished in the summer of 2020th and the data were recently processed. The estimations were performed GAMIT/GLOBK software. All obtained velocities are relative to Eurasia (Dimitrov and Nakov, 2020), (Fig. 1).

After the comprehensive measurement of the geodynamic network in 2020, a new campaign was performed in the summer of 2021. Three additional points were measured – BELM, SATO and LOZ2 (Fig. 2). Point BELM was measured previously in 1997 and 2020, point SATO was measured in 1996 and 2003. Because

the original point LOZE was destroyed after the measurements in 2000, in 2021

we measured the duplicating point LOZ2, which was measured in 1997 but with

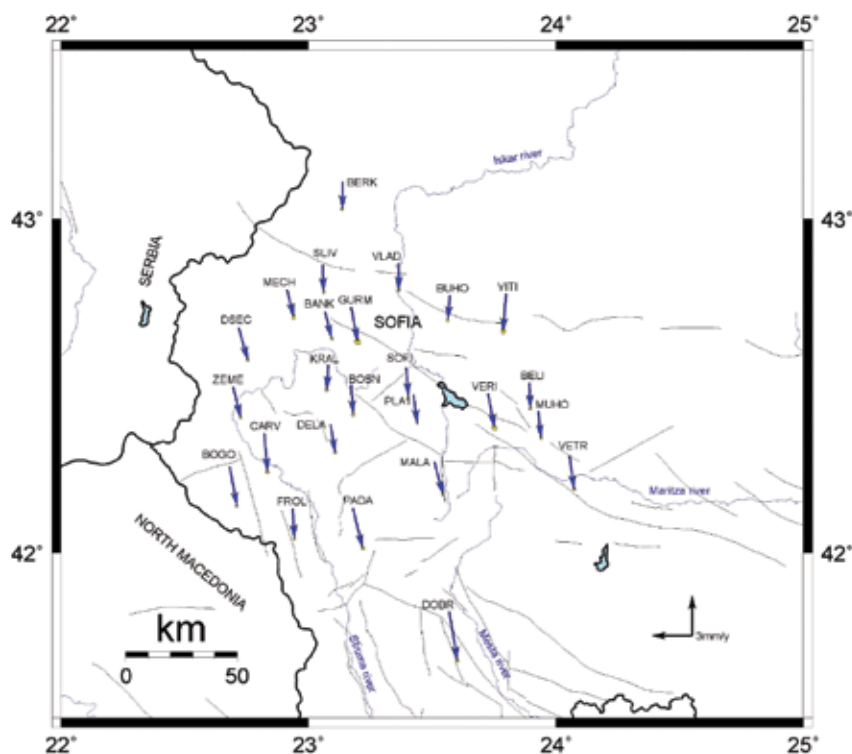


Figure 1. Horizontal velocities relative to Eurasia with main faults, shown as black lines.

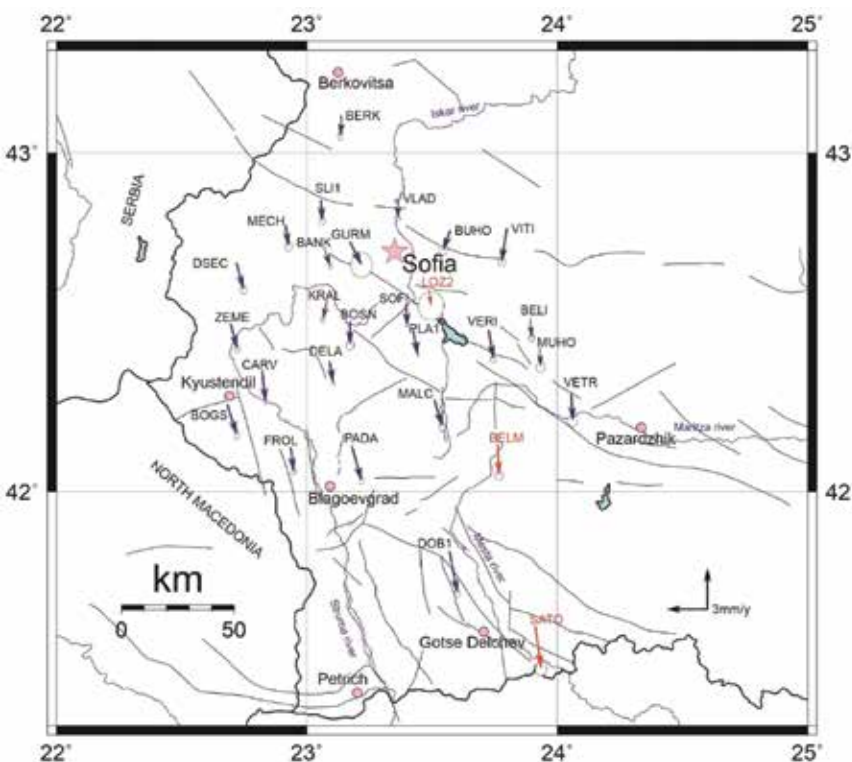


Figure 2. Horizontal velocities relative to Eurasia with main faults, shown as slim lines. The newly observed stations are shown in red.

shorter period of observation. In this reason the obtained result for velocity of this point has greater error, but still is reliable. The measurements are processed and analyzed with the GAMIT-GLOBK software (Herring et al., 2015, Herring et al., 2018). Estimation includes data from campaigns 1997, 2000, 2020 and 2021 years (Dimitrov and Nakov, 2021). The result is velocity vectors shown with an arrow that indicates the direction and speed of GNSS sites. All obtained horizontal velocities are relative to Eurasia (Fig. 2).

Strain rate estimation

For this study all measurements were reprocessed with the GAMIT/GLOBK soft-ware v10.71, to obtain loosely constrained daily solutions saved in SINEX (Solution Independence Exchange format). For estimation of strain rate, the QOCA software (<https://qoca.jpl.nasa.gov/>) is used to model site displacements, which involve all the campaign sites. We use velocities

adjustment in strain rate analysis. Coseismic jumps and post-seismic deformations are removed in the time series. Principal strain axes of the horizontal strain rate tensors are estimated over the Delaunay triangles (Fig. 3).

The preliminary results obtained for the strain rate show that the strain field is not uniform in direction and intensity and creates well-defined single areas with specific characteristics. The rapid change between dominant compression and stretching over short distances is one feature of the deformation field that should be noted (stations MEH-SLI1-GURM-BANK; VERI-BELI-MUHO-VETR; KRAL-BOSN-SOF, etc). The results for strain rates clearly show that presently Sofia graben and its surroundings are subject to a complex deformation and there is not a uniform extensional strain. The area to the north, encompassing stations VLAD, BUHO is under compression [15]. Principal strain axes of the horizontal strain rate tensors estimated over the Delaunay triangles are shown on Figure 3.

Conclusion

The area of Sofia is a moderately active geodynamic area. However, it is exposed at a significant geological hazard, based on the presence of numerous active faults, seismicity, landslides, rockfalls, etc. The area is one of the most important from economical and social points of view of Bulgaria. It hosts important infrastructure and is one of the mostly populated. Acquiring of new geodetic data will allow a better monitoring of geodynamic processes and better evaluation of geodynamics hazards.

The following more important results can be expected from the ongoing project:

- Obtaining estimates of recent crustal movements in the area from Global Navigation Satellite Systems measurements and Synthetic-aperture radar data;
- Determination of the active strain in the region from the results for recent crustal movements. Establishing correlation between earth crust movements, seismic events and tectonic structures;
- Complex analysis of geodetic, geological and seismotectonic information about the territory of Sofia;

The research project can be seen as a new stage in the study of an area with a clear seismic hazard. It is proposed to develop current issues related to the joint interpretation of geodetic, geological and seismotectonic information for the assessment of modern geodynamic processes. The expected results will be a contribution to the assessment of natural risk and seismic hazard in the study area and will have a positive impact for the sustainable development of the region.

Acknowledgements

This paper has been made available with the financial support provided by National Science Fund, call identifier “Competition for financial support of basic research projects – 2019” Project “Monitoring of geodynamic processes in the area of Sofia”. Contract No KII-06-H 34/1.

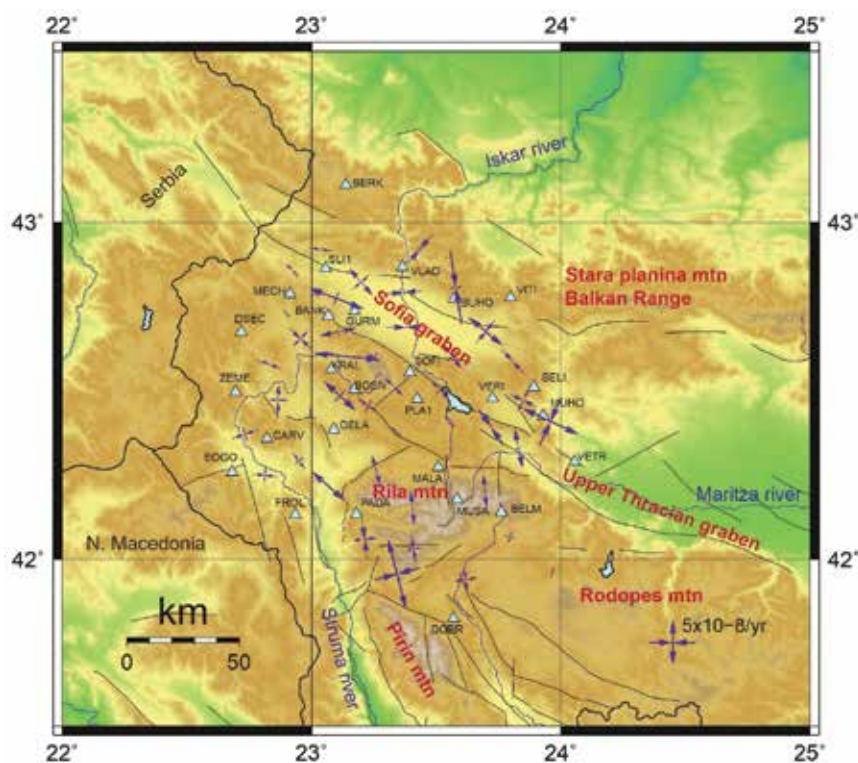


Figure 3. Topography (brown elevated areas, green low lands) and suggested active faults (black lines) with principal axes of the horizontal strain rate tensor (blue arrows).

State-of-art regional geodesy centre on the cards at MNNIT

A state-of-the-art Regional Geodesy Centre (RGC) would soon be set up at Motilal Nehru National Institute of Technology (MNNIT), Prayagraj. Working in close coordination with the country's first National Geodesy Centre (NGC) functioning in Indian Institute of Technology (IIT)-Kanpur, the regional centre would undertake studies in the field of geodesy, tectonic plate motions and monitoring natural hazards such as volcanic, landslide, weather hazards, and climate change, said Dr Ramji Dwivedi, assistant professor, GIS cell of MNNIT.

Besides, it will also contribute to the core research on Earth's shape, size and its gravitational pull, said he who is also principal investigator of this project. "Geodesy is the science of accurately measuring the Earth's size, shape, orientation, mass distribution and how these vary with time and for setting up this regional centre, the department of science and technology (DST) has sanctioned nearly ₹2 crore grant for initial three years," Dwivedi said.

Soon a memorandum of understanding (MoU) will be signed between NCG and RCG at MNNIT Allahabad. He said the regional centre for geodesy would be established in Geographic Information System, MNNIT Allahabad. "The plan is to make the centre fully functional by July," he added. Dwivedi said similar regional centres will also be opened as part of the central government's initiative at IIT-Bombay, ISM-Dhanbad, IIST- Trivandrum, Anna University and MANIT-Bhopal. Dwivedi, who specialises in the field of space geodetic techniques such as GNSS (Global Navigation Satellite System) and InSAR (Interferometric synthetic aperture radar), said the regional centre will provide information about area of mapping, remote sensing in new technology. "Various types of equipment will be procured as part of this initiative which will be used to monitor surface deformation," he said.

It is proposed to develop current issues related to the joint interpretation of geodetic, geological and seismotectonic information for the assessment of modern geodynamic processes

References

Burchfiel, B. C., R. Nakov, Tz. Tzankov, L. H. Royden (2000). Cenozoic extension in Bulgaria and northern Greece: The northern part of the Aegean extensional regime: in Bozkurt, E., Winchester, J. A., and Piper, J. D. A., (eds), *Tectonics and Magmatism in Turkey and the Surrounding Area: Geological Society Special Publication No. 173*, p. 325-352.

Tzankov, Tz., D. Angelova, R. Nakov, B. C. Burchfiel, L. Royden (1996). The Sub-Balkan graben system of central Bulgaria. *Basin Research*, 8, 125-142.

Yosifov, D., I. Paskaleva, E. Botev, B. Rangelov (2018) The seismic risk for Sofia. *NTS MDGM*, S., 207. (In Bulgarian).

Radulov, A., M. Yaneva, S. Shanov, K. Kostov, V. Nikolov, N. Nikolov (2012). Coseismic geological effects related to the May 22, 2012 Pernik earthquake, Western Bulgaria. In: *Proceedings of the National Conference "Geosciences 2012"*, Bulgarian Geological Society, Sofia, 121-122.

Kotzev, V., R. Nakov, B.C. Burchfiel, N. Dimitrov (2005). Crustal motion in Central West Bulgaria from triangulation and GPS data. *C.R. Acad. Bulg. Sci.*, 58, 6, 699-704.

Kotzev, V., R. Nakov, B. C. Burchfiel, R. W. King. (2001). GPS constraints on the kinematics of southwestern Bulgaria. - *C. R Acad. Bulg. Sci.*, 54, 7, 51-54.

Kotzev, V., R., Nakov, Tz., Georgiev, B.C., Burchfiel, R.W., King (2006). Crustal motion and strain accumulation in western Bulgaria. – *Tectonophysics*, 413 (3-4), 27-145.

Herring, T. A., R. W. King, M. A. Floyd, S. C. McClusky. 2018. *GAMIT reference manual, GPS Analysis at MIT, Release 10.7*. Cambridge, MA: Massachusetts Institute of Technology.

Herring, T. A., M. A. Floyd, R. W. King, S. C. McClusky. 2015. *GLOBK reference manual, Global Kalman filter VLBI and GPS analysis program, Release 10.6*. Cambridge, MA: Massachusetts Institute of Technology.

QOCA Homepage, <https://qoca.jpl.nasa.gov/>, last accessed 2021/06/06.

Dimitrov N, R. Nakov. (2020). Recent GPS results on the geodynamics of the area around Sofia (Central-Western Bulgaria). *Review of the Bulgarian Geological Society*, 3, 81, 2020, ISSN: 0007-3938, 241-243.

Dimitrov N., R. Nakov. (2021). Supplementary measurements in the Sofia Geodynamic Network. Significance for contemporary local and regional geodynamics. *Review of the Bulgarian Geological Society*, 82, 3, 239-241; <https://doi.org/10.52215/rev.bgs.2021.82.3.23>.

Dimitrov N, I. Georgiev, Nakov R. (2020) Monitoring of geodynamic processes in the area around Sofia. *SGEM*, Volume 20, Book 2.2, 18-24 August, Albena, Bulgaria, ISBN:978-619-7603-07-1, ISSN:1314-2704, DOI:10.5593/sgem2020/2.2/s09.010, p 79-86.

Spatial analysis of soil trace element contaminants in urban public open space

The results of the study conducted in Perth, Australia show distinct advantages of using spatial statistics at the site investigation scale, and for measuring multiple elements not just potential contaminants



Andrew W. Rate
School of Agriculture
and Environment, The
University of Western
Australia, Australia

Abstract

Public recreation areas in cities may be constructed on land which has been contaminated by various processes over the history of urbanisation. Charles Veryard and Smith's Lake Reserves are adjacent parklands in Perth, Western Australia with a history of horticulture, waste disposal and other potential sources of contamination. Surface soil and soil profiles in the Reserves were sampled systematically and analysed for multiple major and trace elements. Spatial analysis was performed using interpolation and Local Moran's I to define geochemical zones which were confirmed by means comparison and principal components analyses. The degree of contamination of surface soil in the Reserves with As, Cr, Cu, Ni, Pb, and Zn was low. Greater concentrations of As, Cu, Pb, and Zn were present at depth in some soil profiles, probably related to historical waste disposal in the Reserves. The results show distinct advantages to using spatial statistics at the site investigation scale, and for measuring multiple elements not just potential contaminants.

1. Introduction

A number of studies have documented the potential for contaminant additions to soils from a range of urban activities. Horticultural activities are known to leave a legacy of soil contamination related to use of fertilisers, manures, and

other materials [1-3]. The disposal of metalliferous and other wastes is known to cause soil contamination with trace elements [4]. Excavation of peaty and/or sulfidic subsoils is known to result in contamination of soils with acidity and metals [5,6]. Public facilities such as vehicle and storage depots and electrical substations are also potential contaminant sources known to have caused soil pollution [7,8]. Finally, building construction is a likely source of soil, sediment, and water contamination [9].

Smith's Lake and Charles Veryard Reserves are public recreation spaces in metropolitan Perth, Western Australia (WGS84 115.8505 °E, 31.9319 °S), with a complex history of land use change that is typical of many urban areas worldwide [10].

Spatial statistical techniques present useful tools for identifying and describing soil contamination. For example, the use of variogram and/or spatial autocorrelation analysis can be used to quantify the degree of spatial dependence between contaminant concentrations in soil samples [11]. In addition, use of local spatial autocorrelation statistics such as Local Moran's I can be used to categorize locations, or clusters of locations, using the statistical significance and the magnitude of the response variable, such as in LISA (Local Indicators of Spatial Association) analysis [12]. Use of these techniques to study urban soil contamination has been limited so far

to citywide spatial scales (tens of kilometers), covering multiple current land uses [11,13,14]. On whole-city scales, clusters of positively autocorrelated samples with higher concentrations are interpreted to represent “regional hotspots” of contamination. Conversely, isolated samples of higher concentration showing negative autocorrelation with surrounding low-concentration samples (“high-low” points in the LISA framework) are interpreted as being “isolated hotspots”, potentially caused by point sources [14]. Very few published studies have used autocorrelation statistics to analyse spatial patterns of soil contamination at scales of a few hundred metres, with a single or restricted range of land use, which are typical of environmental site investigations where contamination is suspected. At smaller spatial scales, a reasonable hypothesis is that clusters of positively autocorrelated, high concentration points (“high-high” points in LISA) are more likely to represent point source contamination, whereas isolated “high-low” points will have less significance.

This study therefore had multiple objectives. The potential contaminants of primary interest were the trace elements As, Cr, Cu, Ni, Pb, and Zn, due to their known effects on human health and ecosystem functioning. This set of elements is relevant to urban soil contamination in many cities globally, and also represents a range of geochemical behaviour with As and Cr often existing as oxyanions in soils in contrast to the cationic metals Cu, Ni, Pb, and Zn. In addition, a range of mobilities would be expected, with Cr and Pb commonly showing low mobility in soils in contrast with Zn and As which are usually more mobile. The major elements Al, Ca, and Fe, and soil pH and EC, were of interest to support and explain the trace element data. The scientific objectives, therefore, were first: to characterize the concentrations and spatial distributions of potential contaminants in soil in the Smith’s Lake and Charles Veryard Reserve area. The second objective was to identify any

spatial patterns in the data over scales of a few hundred metres, and match these to the known history of the sites. The final aim was to evaluate the findings from spatial analysis of surface sampling as indicators of subsoil contamination. The research approach evaluates the utility of spatial analysis to provide more quantitative evidence of zones of contamination in urban soils, and should therefore be applicable to other urban soil environments at similar spatial scales.

2. Materials and methods

2.1 Study site

Smith’s Lake and Charles Veryard Reserves are situated in the historical location of Three Island Lake and associated water bodies, on land that was drained from the 1870s to allow the establishment of horticulture. The area has experienced multiple land uses, including market gardening (1920s-1950s), dumping of rubbish, and recreation/parkland [15]. The Claise Brook Main Drain was changed from an open drain to an underground stormwater pipe in the mid-1970s, and the present Smith’s Lake was also constructed as a stormwater compensating basin at this time. The 1970s were also a time of substantial residential development in this area. The 2000s saw urban gentrification and infill occurring in the area; a local government Depot to the east of Smith’s Lake Reserve was redeveloped to residential land in 2000-2002. A large sports centre building in the south of Smith’s Lake Reserve was demolished and rehabilitated to parkland in 2008, with conversion of some larger residential lots to allow construction of higher density housing also occurring around 2008.

While the land around Smith’s Lake Reserve is currently residential, several previous facilities and activities adjacent to the current reserve had the potential to modify fluxes of a range of contaminants. These include the land uses described above, and: the burial of the Claise Brook

Main Drain, the Council Works Depot and its subsequent redevelopment, the demolition and rehabilitation of the sports centre, and the electrical supply substation constructed in the 1960s (and upgraded in 2001) adjacent to the north-west corner of the reserve. Smith’s Lake itself was rehabilitated by a community group in 1999 [16], with construction of a path approximating the line of the underground main drain in 2010-2011. Floodlight pylons were installed in Charles Veryard Reserve in 2016, involving excavation of potential acid sulfate soil material (based on maps from [17]).

2.2 Sampling

Sampling of soil at Smith’s Lake and Charles Veryard Reserves was conducted on two occasions: in March 2017 (a grid of surface samples) and March 2018 (profile sampling at selected locations). In 2017, surface soil sampling locations were pre-selected prior to sampling using a randomised-within-grid sampling strategy (Figure 1) using a 52 × 52 m grid to maximise site coverage, and two samples per grid square, with the objective of sampling the grassed areas within the Reserves without statistical bias. In the field, preselected sample locations were located using handheld GPS. If randomised sample coordinates were too close to paved surfaces, water, structures, *etc.*, the location was moved by approximately 5 m and the revised coordinates were recorded.

Surface soil was sampled in cylindrical cores from 0-10 cm depth using a stainless steel corer. Triplicate cores at each location were bulked to achieve a sample mass of *ca.* 500 g, and stored in zip-lock plastic bags prior to transport back to the laboratory. Soil sample cavities were re-filled with clean soil supplied by the sampling team.

In 2018, a second sampling of soil profiles to up to 100 cm depth was conducted using Garret-style augers. Separate samples were collected for each of 8 profiles (Figure 1) in 10 cm depth increments.

Soil samples were air-dried in a laminar air-flow drying cabinet at 40 °C and sieved through a 2 mm aperture prior to analysis.

2.3 Chemical analysis

The electrical conductivity (EC; proportional to soluble salt content) of soil samples was determined on 1 : 5 solid : deionised water suspensions using a calibrated conductivity cell electrode. The pH was measured on the same suspensions using a glass-reference pH electrode after a 2-point buffer calibration [18].

The near-total concentrations of 26 elements (Al, As, Ba, Ca, Cd, Ce, Cr, Cu, Fe, Gd, K, La, Mg, Mn, Mo, Na, Nd, Ni, P, Pb, S, Sr, Th, V, Y, and Zn) were measured on samples by inductively-coupled plasma optical emission spectrometry (ICP-OES) following digestion of soil in concentrated nitric and hydrochloric acids (*i.e. aqua regia*) at ca. 130 °C [19]. Aqua regia digestion is commonly used to determine environmentally significant concentrations, since it largely excludes elements within the matrices of silicates and other recalcitrant minerals. Before acid digestion, samples were ground to $\leq 50 \mu\text{m}$ using ceramic mortars and pestles. Reagent blanks, and grinding blanks composed of acid-washed silica sand, were included in analytical runs to check for contamination. The standard reference stream sediment material STSD2 [20] was analysed identically to samples to assess analytical accuracy. Measurement precision was assessed using analytical duplicates on ca. 10% of samples.

The lower limits of analytical detection were calculated, where possible, from $3 \times$ the standard deviation of multiple reagent blank concentrations [21]. Concentrations lower than mean blank values, or below calculated lower detection limits, or both, were deleted from the dataset.

2.4 Statistical and numerical analysis

Data management and transformation of variables was conducted using Microsoft Excel®. Statistical and graphical analyses of data were

performed in the statistical computing environment ‘R’ [22] and associated packages. Skewed variables (identified with the Shapiro-Wilk test for normality) were \log_{10} -transformed, or power-

transformed based on the Box-Cox algorithm, and re-checked for normality.

A general inability of variables to be transformed to yield normal distributions

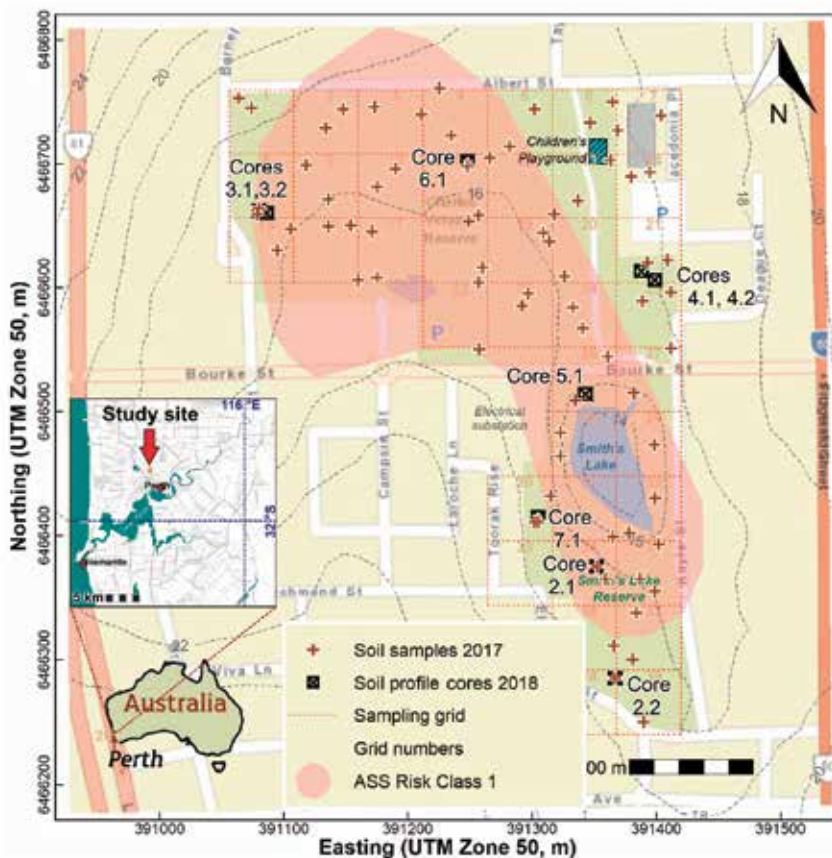


Figure 1. Street map showing soil sampling locations, and the initial grid used for sampling design, at Smith's Lake and Charles Veryard Reserves. Contours are land elevations in metres; the pale red polygon shows moderate to high acid sulfate soil (ASS) risk.

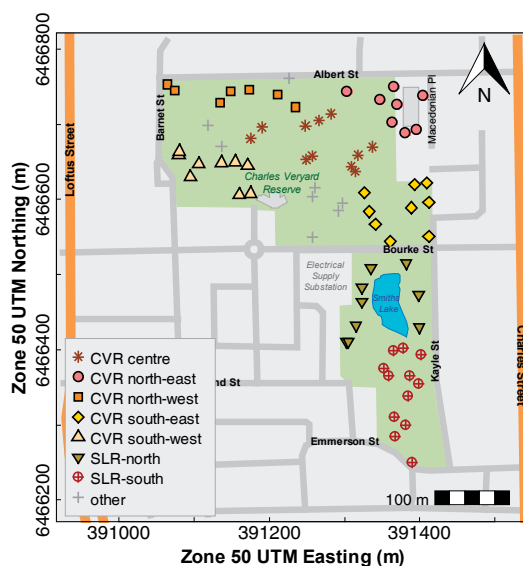


Figure 2 Simplified map showing sampling zones at Smith's Lake and Charles Veryard Reserves. CVR is Charles Veryard Reserve; SLR is Smiths Lake Reserve.

dictated the use of the non-parametric Spearman correlations, and Wilcoxon or Kruskal-Wallis tests for mean comparisons. If Kruskal-Wallis tests showed a significant difference, the R package ‘PMCMR’ [23] was used to apply the post-hoc Conover’s test for pairwise comparisons of mean rank sums. Simple regression models were fitted using the \log_{10} -transformed variables. The potentially misleading effects of compositional closure were addressed using transformations to centred log-ratios [24], which were used for principal components analyses. Principal components analyses were conducted using only variables having minimal or no missing observations.

Distribution maps were constructed using the ‘OpenStreetMap’ package [25] with elevation contours interpolated from a dense grid of land elevations from Google [26] generated using the R package ‘googleway’ [27] and interpolated using the R package ‘akima’ [28]. Spatial autocorrelations were assessed using global and local Moran’s I statistics, calculated using the R package ‘ltools’ [29]. Local Moran’s I values showing significant association ($p \leq 0.05$) were categorised using high-low notation, based on the point measurement relative to the median and the sign of the Local

Moran’s I statistic. Spatial interpolations were achieved using an inverse distance weighting method using the R packages ‘sp’ [30] and ‘gstat’ [31]. Preliminary analysis showed that inverse-distance interpolation gave similar results to simple kriging, but kriging interpolation was not used, based on the requirement of ≥ 100 observations to generate a reliable experimental variogram [32].

A composite estimate of soil contamination was calculated from the concentrations of As, Cu, Pb, and Zn as the Integrated Pollution Index, IPI [33], shown in Equation 1:

$$IPI = \left(\sum_{i=1}^n \left(\frac{C_i}{S_i} \right) \right) / n, \quad (1)$$

In Equation 1, \sum means the sum of terms 1 to n, C_i = the measured concentration of i^{th} element, S_i = the background concentration of i^{th} element, n = the number of elements. The S_i values used (in mg/kg: As=1.5, Cr=10, Cu=2, Pb=5, Zn=6) were published ambient background concentrations for the Perth region [34], but this report suggests a zero background concentration for Ni. In this study 1 mg Ni/kg was used for background, which is the lowest (most conservative) 25th percentile concentration among similar datasets (e.g. [35]).

3. Results

3.1 Bulk chemical analyses of surface soil

Substantial variability in the concentrations of most elements, including potential contaminants, was observed in surface soils at Smith’s Lake and Charles Veryard Reserves (Table 2). In most cases, the maximum concentrations were at least 5 times the minima. Much greater variability was observed for calcium (Ca, maximum/minimum ≈ 108); cadmium (Cd), copper (Cu), magnesium (Mg), manganese (Mn), neodymium (Nd), nickel (Ni), phosphorus (P), lead (Pb), sulfur (S), strontium (Sr), and zinc (Zn) all had maximum/minimum ratios between 20 and 90. Soluble salt content measured by EC showed a maximum/minimum ratio of ≈ 29 , and there was a relatively large, ≈ 3.4 unit, range in pH across the Reserves. Except for zinc, which exceeded the interim Ecological Investigation Level (EIL; National Environment Protection Council, 1999) in 3 samples, no other soil thresholds were exceeded by any element.

3.2 Spatial distributions in surface soil

The measurements of primary interest (pH, EC, Al, As, Ca, Cu, Fe, Pb, Zn) generally

Table 1. Summary of pH, EC, and major element concentrations in surface (0–10 cm) soil and in vertical soil profile samples at Smith’s Lake and Charles Veryard Reserves. EC and pH were measured in 1:5 solid : deionised water suspensions; element concentrations were measured using *aqua regia* digestion followed by ICP-OES.

Statistic	pH	EC ($\mu\text{S}/\text{cm}$)	Major element concentration (mg/kg)							
			Al	Ca	Fe	K	Mg	Na	P	S
<i>Surface soil (random-in-grid samples, 2017)</i>										
Mean	6.92	183	2667	5083	2695	161	425	130	244	309
Std. Dev.	0.63	146	758	7082	939	75.3	285	69	123	186
Minimum	5.28	29.1	396	283	1205	41.1	57.3	27.8	18.5	43
Median	6.84	151	2637	1813	2530	150	347	118	221	280
Maximum	8.63	835	4722	30472	5640	424	1471	410	596	1293
No of valid analyses	73	58	68	68	68	68	68	68	68	68
<i>Soil profiles to ≤ 100 cm (2018)</i>										
Mean	7.67	116	3214	11061	4430	173	548	148	146	518
Std. Dev.	1.96	61	2168	14254	3358	100	505	100	137	334
Minimum	4.48	7.92	149	38	218	26	14	11	4	48
Median	7.98	83	2880	7894	3593	134	450	127	140	293
Maximum	9.40	860	10353	57265	22180	655	2365	513	386	4929
No of valid analyses	84	83	85	85	85	85	85	85	85	83

showed significant overall spatial patterns across the study area, shown by p values ≤ 0.05 for Global Moran's I. The exceptions were Al, Ca, Cr, and Ni for which the Global Moran's I values were close to zero (Table 3). The spatial patterns and clusters of points with significant local autocorrelation are shown in Figure 3 to Figure 6, and summarised in Table 3.

Arsenic (As) showed a broad peak in concentration in soil in the south-east of Charles Veryard Reserve, with scattered local maxima in As concentration in a few other locations (Figure 3). The As peak in the south-east of Charles Veryard Reserve was co-located with samples having significant ($p \leq$

0.05) high-high local Moran's I. Two points in Smith's Lake Reserve had significant low-high local Moran's I (*i.e.* isolated low As concentrations).

Copper (Cu) showed peaks in the north-east and south-east of Charles Veryard Reserve, with no other obvious maxima (Figure 3). Samples in both peaks in

Table 2. Summary of minor/trace element concentrations in surface (0–10 cm) soil and in vertical soil profile samples at Smith's Lake and Charles Veryard Reserves. Element concentrations were measured using *aqua regia* digestion followed by ICP-OES.

Statistic	Concentrations (mg/kg)											
	As	Ba	Cd	Cr	Cu	Mn	Mo	Ni	Pb	Sr	V	Zn
<i>Surface soil (random-in-grid samples, 2017)</i>												
Mean	2.58	15.7	0.11	7.33	8.69	39.5	0.23	2.58	25.7	27.8	5.38	55.2
Std. Dev.	1.09	7.38	0.1	2.29	11	23.7	0.1	2.83	31.7	40.3	1.66	56.5
Minimum	0.9	6.2	0.02	1.17	2.13	2.68	0.07	0.25	3.23	2.4	1.28	5.59
Median	2.3	14.5	0.08	7.32	5.25	34.5	0.22	2.13	14.7	10.3	5.35	34.7
Maximum	5.86	41.7	0.66	13.8	67.5	127	0.6	21.3	174	186	10.6	304
No of analyses	68	68	62	68	68	68	68	68	68	68	68	68
No > HIL(C) ¹	0	–	0	0	0	0	–	0	0	–	–	0
No > EIL ³	0	0	0	0	0	0	–	0	0	–	0	3
<i>Soil profiles to ≤ 100 cm (2018)</i>												
Mean	3.28	25.2	0.18	9.09	41.4	28.0	0.48	5.39	72.7	62.3	8.38	117
Std. Dev.	2.79	26.2	0.31	6.96	66.6	21.7	0.81	20.7	98.8	85.1	5.56	191
Minimum	0.6	1.9	0.01	0.2	2.8	1.5	0.06	0.6	3.5	1.8	0.3	3.3
Median	2.5	15.3	0.06	8.1	15.1	24.3	0.21	1.97	32.2	34.3	7.2	43.2
Maximum	14.6	139	1.6	34.4	356	97.9	5.63	181	568	391	30.4	1155
No of analyses	83	85	79	85	67	85	78	75	84	80	85	84
No > HIL(C) ¹	0	–	0	0	0	0	–	0	0	–	–	0
No > EIL ³	0	0	0	0	8	0	–	1	1	0	0	14

¹Health Investigation Level C (Recreational) [36]; ³Ecological Investigation Level (interim urban) [37].

Table 3. Global Moran's I, P-values simulated by Monte-Carlo randomization, and information on local spatial autocorrelation for the variables of principal interest in surface soil at Smith's Lake and Charles Veryard Reserves. Variables except pH were log₁₀-transformed before calculation. IPI is integrated pollution index (Eq. 1).

Variable	Moran's I	P-value	Number of points with significant Local Moran's I	Location (and number of points) of high-high Local Moran's I clusters a
pH	0.440	>0.001	13	CVR-SW (2), CVR-SE (3), SLR-S (4)
EC	0.157	0.035	7	SLR-S (3)
Al	0.014	0.691	4	CVR-SE (2) b
As	0.228	0.002	6	CVR-SE (4)
Ca	0.074	0.254	6	SLR-S (2)
Cr	0.016	0.672	4	CVR-SE (1)
Cu	0.331	>0.001	9	CVR-NE (3), CVR-SE (5)
Fe	0.142	0.044	11	CVR-NE (1), CVR-SE (5)
Ni	0.047	0.426	5	CVR-SE (1) b
Pb	0.324	>0.001	11	CVR-SE (5), SLR-N (2)
Zn	0.209	0.004	10	CVR-NE (2), CVR-SE (4)
IPI	0.257	>0.001	10	CVR-NE (1), CVR-SE (5)

^a CVR is Charles Veryard Reserve; SLR is Smiths Lake Reserve; NE is north-east; NW is north-west; SE is south-east; SW is south-west; N is north; S is south; E is east; ^b not associated with main CVR-SE cluster.

Cu concentration were significantly spatially autocorrelated (high-high, local Moran's $I_p \leq 0.05$). One point in

north-west Charles Veryard Reserve had significant low-high local Moran's I (i.e. an isolated low Cu concentrations).

Lead (Pb) showed peaks in concentration in soil in the south-east of Charles Veryard Reserve and the north of Smith's Lake

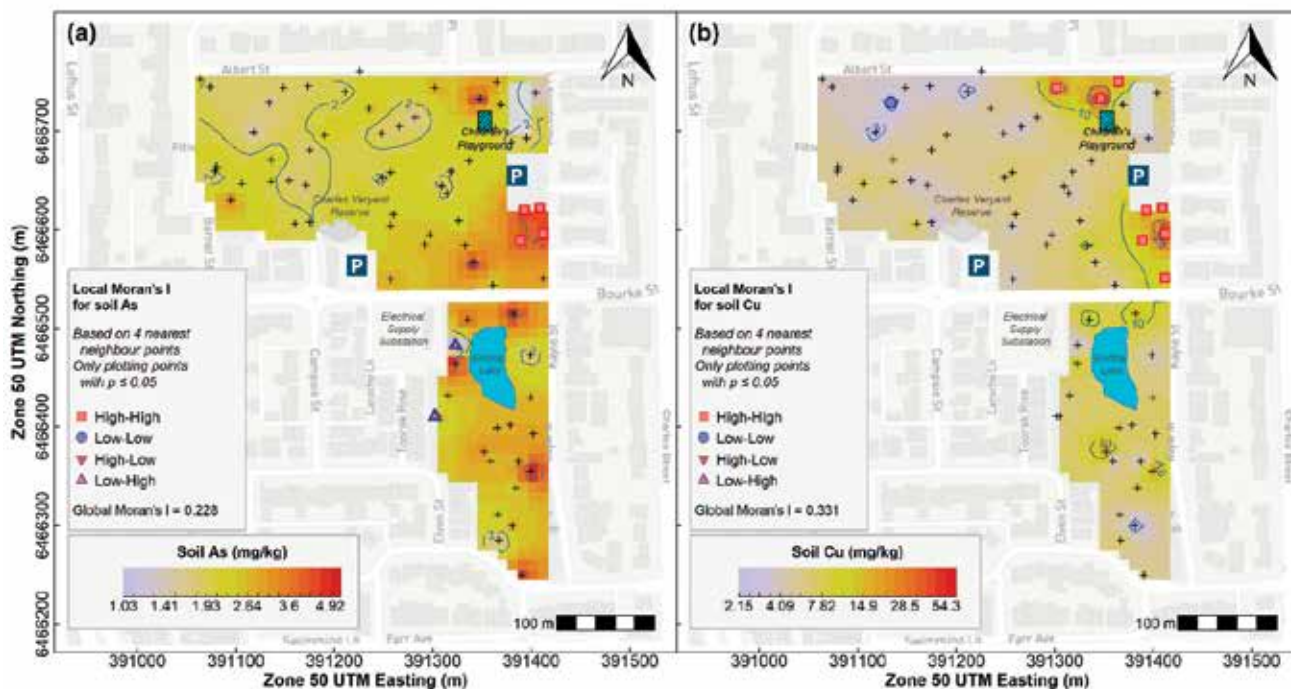


Figure 3. Spatial distributions of (a) As and (b) Cu in soil across Smith's Lake and Charles Veryard Reserves, interpolated by inverse distance weighting with significant local spatial autocorrelations (Local Moran's $I \leq 0.05$) indicated with filled symbols. All sample points shown by + symbols

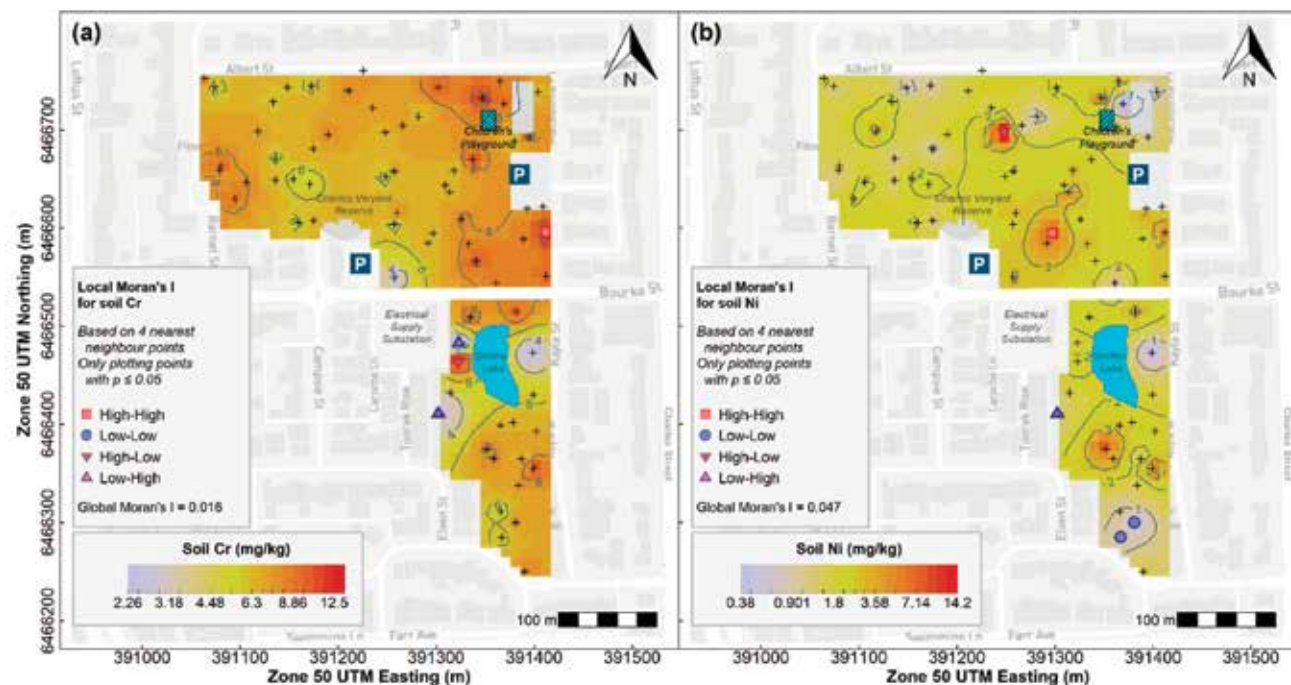


Figure 4. Spatial distributions of (a) Cr and (b) Ni in soil across Smith's Lake and Charles Veryard Reserves, interpolated by inverse distance weighting with significant local spatial autocorrelations (Local Moran's $I \leq 0.05$) indicated with filled symbols.

Reserve, with scattered local maxima in Pb concentration in a few other locations

(Figure 5). The Pb peak in the south-east of Charles Veryard Reserve was co-

located with samples having significant ($p \leq 0.05$) high-high local Moran's I. A broad

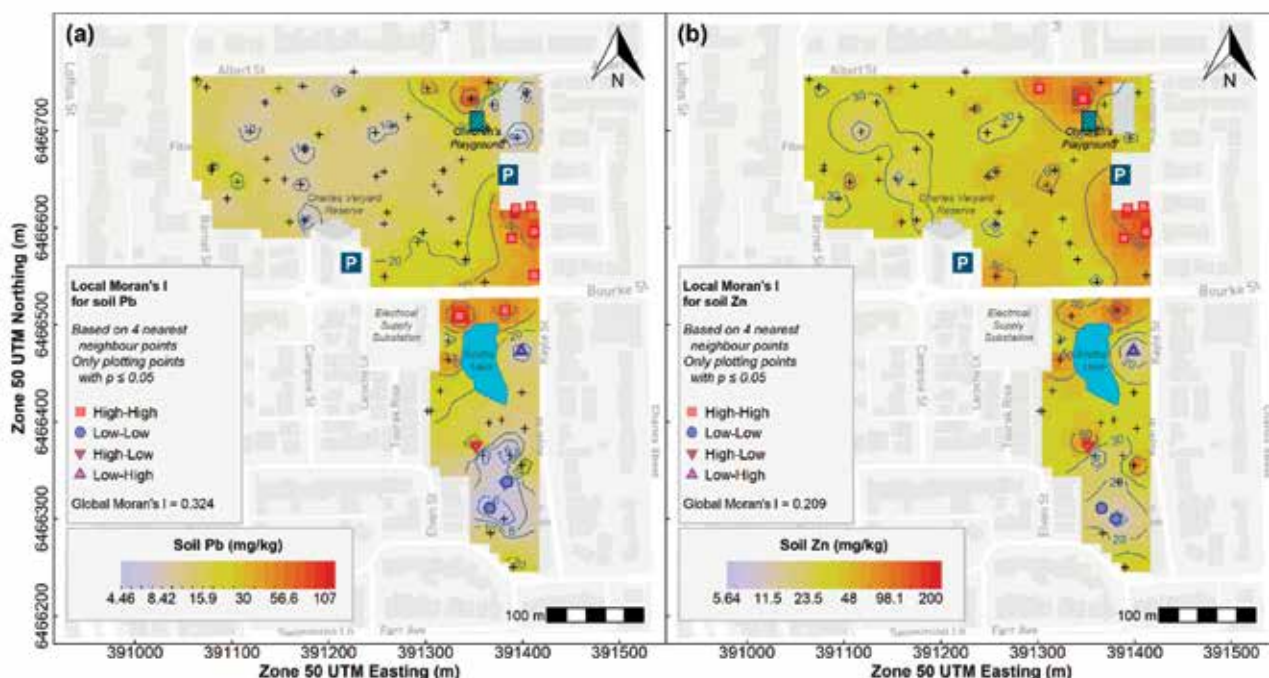


Figure 5. Spatial distributions of (a) Pb and (b) Zn in soil across Smith's Lake and Charles Veryard Reserves, interpolated by inverse distance weighting with significant local spatial autocorrelations (Local Moran's $I \leq 0.05$) indicated with filled symbols. All sample points shown by + symbols.

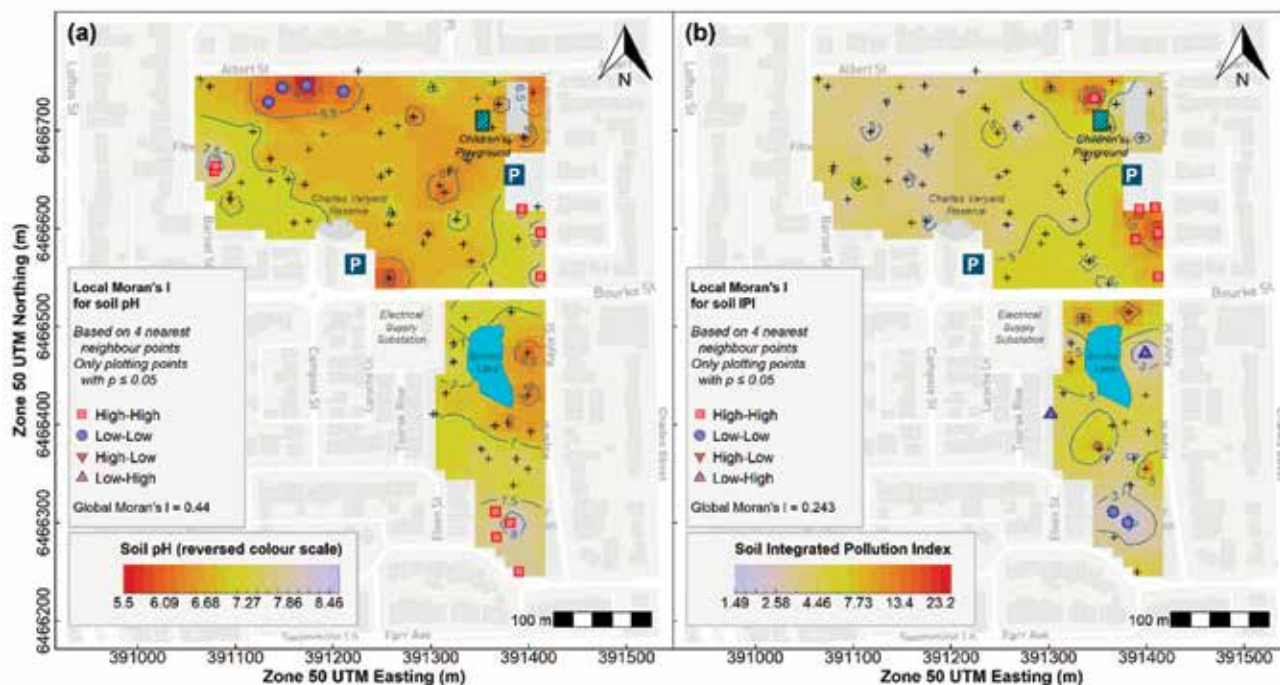


Figure 6. Spatial distributions of (a) pH and (b) Integrated Pollution Index (IPI) in soil across Smith's Lake and Charles Veryard Reserves, interpolated by inverse distance weighting with significant local spatial autocorrelations (Local Moran's $I \leq 0.05$) indicated with filled symbols. All sample points shown by + symbols.

area of low Pb concentrations in Smith's Lake Reserve coincided with significant ($p \leq 0.05$) low-low local Moran's I, and instances of significant high-low and low-high local Moran's I values represented isolated high and low Pb concentrations.

Zinc (Zn) showed peaks in the north-east and south-east of Charles Veryard Reserve, with a few other subtle maxima (Figure 5). Samples in both clear peaks in Zn concentration were significantly spatially autocorrelated (high-high, local Moran's I $p \leq 0.05$). An area of low Zn concentrations in Smith's Lake Reserve coincided with significant ($p \leq 0.05$) low-low local Moran's I. Similar to Pb, instances of significant high-low and low-high local

Moran's I values in Smith's Lake Reserve represented isolated high and low Zn.

Soil pH showed a cluster of lower values in the north-west of Charles Veryard Reserve with significant low-low spatial autocorrelation (Moran's I $p \leq 0.05$). In contrast, significant clusters of higher pH values were present in the west of Charles Veryard Reserve, the south-east of Charles Veryard Reserve, and the south of Smith's Lake Reserve (Figure 6).

Finally, the derived Integrated Pollution Index (IPI) had a maximum in the south-east of Charles Veryard Reserve, with a minor maximum in the north-east (Figure 6). A cluster of samples in the south-

east IPI peak were significantly spatially autocorrelated (high-high, local Moran's I $p \leq 0.05$). An isolated low IPI value (low-high local Moran's I, $p \leq 0.05$) was present to the east of Smith's Lake.

3.3 Relationships between soil elements

Several significant positive correlations existed between elements across the soil data from Charles Veryard and Smith's Lake Reserves (Table S1, supplementary material). Calcium, Mg and Sr were very highly correlated ($r=0.80-0.96$), and Ca and Sr were the only elements significantly correlated ($r=0.66$) with pH. The major elements Na, K, and Mg were all highly correlated ($r \geq 0.7$), as were P, K, Mn, and S. High correlations also existed between iron (Fe) and As, Ba, Cu, Pb, and V. Many potential contaminants were also highly correlated with one another, e.g.: Cu with Ba, Pb, and Zn; Pb with Cd, Cu, and Zn; Cr with V.

Principal components analysis (Figure 7) showed grouping of Cu, Pb, and Zn in PC1-PC2 space, associated with some of the samples from north-east and south-east where peak concentrations of these elements were observed (Figure 3, Figure 5). Arsenic plots at similar values of PC2, but has an association with Fe and Cr at small positive PC1 values. No obvious element associations were

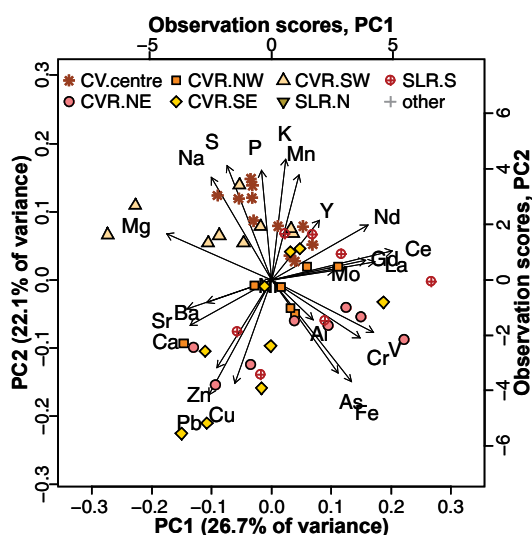


Figure 7. Principal components biplot for the first two principal components based on elemental composition in surface soil at Charles Veryard and Smith's Lake Reserves. Observation scores are identified by sampling Zone (see Figure 2). Concentrations were transformed using centered log-ratios before PCA, to avoid spurious effects of compositional closure.

Table 4. Comparison of pH, EC (1:5 soil:water extract), element concentrations, and IPI in distinct Zones of Smith's Lake (SLR) and Charles Veryard (CVR) Reserves. Mean values in a row are different if no superscripts are shared ($p \leq 0.05$, Conover's pairwise test with Holm's correction).

Variable	P (K-W) ¹	Mean in each zone ²							
		CVR-centre	CVR-NE	CVR-NW	CVR-SE	CVR-SW	SLR-N	SLR-S	other
pH	0.0001	6.58a	6.65ab	6.24a	7.34bc	7.35bc	6.88abc	7.38c	6.66abc
EC	0.013	155ab	90.7ab	273a	159ab	232a	68.1b	265ab	143ab
Al	0.028	2530ab	2857ab	2285a	3373b	2621ab	1960ab	3011ab	2489ab
As	0.004	1.91a	2.46ab	1.96a	3.79b	2.17a	2.99ab	3.04ab	2.38ab
Ca	0.004	1766abc	3511abc	4534abc	6710abc	7472ab	3570ac	11450b	1343c
Cr	0.020	6.98ab	8.47ab	6.62a	9.42b	7.18ab	5.85ab	7.51ab	6.20a
Cu	0.010	5.10ab	16.7ab	3.57a	17.6b	5.36ab	8.43ab	8.34ab	4.52ab
Fe	0.041	2377ab	2936ab	2071a	3623b	2418ab	2680ab	2861ab	2535ab
Ni	0.300	ns	ns	ns	ns	ns	ns	ns	ns
Pb	0.043	11.7a	31.2ab	15.4ab	56.9b	15.3ab	47.8ab	15.7a	16.5ab
Zn	0.255	ns	ns	ns	ns	ns	ns	ns	ns

¹Overall p-values from Kruskal-Wallis test; ²CVR is Charles Veryard Reserve; SLR is Smiths Lake Reserve;

NE north-east; NW north-west; SE south-east; SW south-west; N north; S south.

observed using PCA for Ni. The principal components analysis also identifies an association of Ca with Sr and Ba, an association of nutrient elements (S, P, K) with the central Charles Veryard Reserve samples, and clustering of rare-earth and related elements (Ce, Gd, La, Nd, Y). Additional results derived from principal components analysis are available in the Supplementary Materials.

In surface soil, there was a weak negative relationship between lead and vanadium concentrations and minimum (Euclidean) distance from any road

surrounding or bisecting the reserves (Figure 8). No other contaminant of primary interest showed a significant trend in relation to distance from roads.

3.4. Depth distributions of As, Cr, Cu, Ni, Pb, and Zn

Depth profile plots for As, Cr, Cu, Ni, Pb, and Zn are presented in Figure 9, Figure 10 and Figure 11. Depth profiles of As, Cr, Cu, Ni, Pb, and Zn frequently showed maximum concentrations in subsurface soil samples. High maximum concentrations of Pb (376 mg/kg) and

Zn (1155 mg/kg) were measured at 30–40 cm in core 4.2 (Figure 11), on the eastern side of Charles Veryard Reserve south of the Macedonia Place car park. Core 3.2 also contained 568 mg/kg Pb at 50–60 cm. Core 4.2 also contained the maximum concentration of As (14 mg/kg at 20–30 cm), Cd, Mn, and Ni. The greatest concentration of Cu (356 mg/kg) was observed in the adjacent core 4.1 (Figure 9). There was a tendency for pH to increase with increasing depth, and EC to decrease with increasing depth, and the trends in Fe with depth were very similar to those for As (Figure S1, supplementary material).

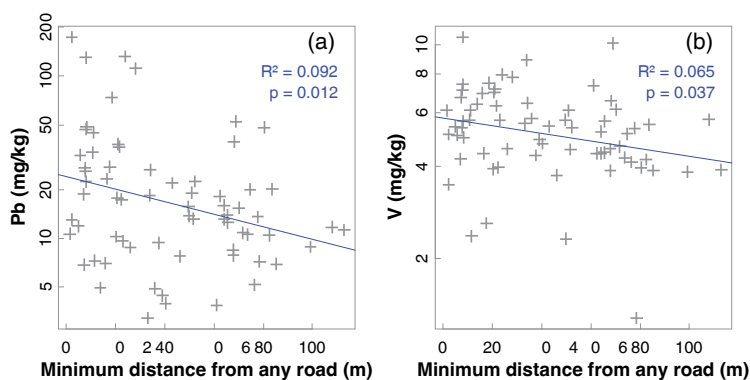


Figure 8. Weak trends in (a) Pb and (b) V concentrations in surface soil with distance from roads in Charles Veryard and Smith’s Lake Reserves. Solid blue lines are log-linear models.

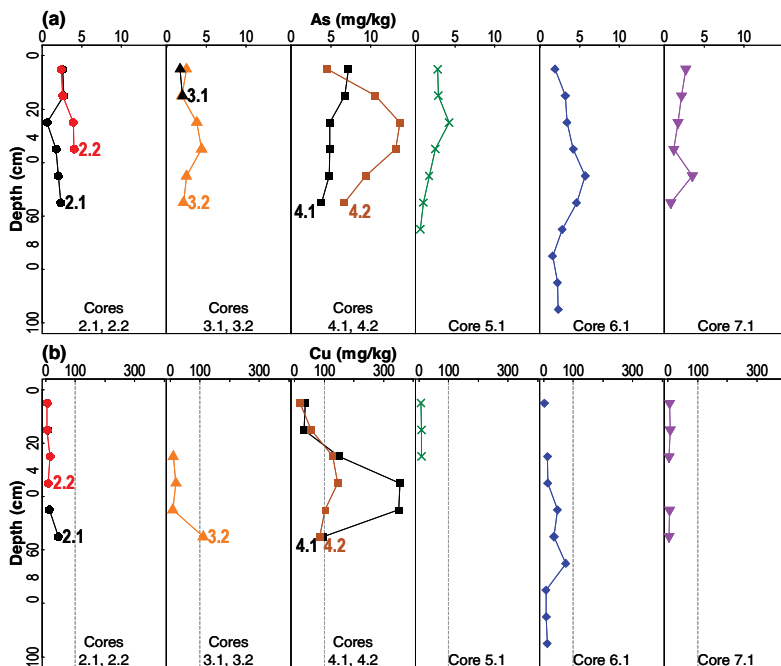


Figure 9. Depth profiles of (a) arsenic (As) and (b) copper (Cu) in soil cores collected from Smith’s Lake and Charles Veryard Reserves, City of Vincent, Western Australia. Core locations from Figure 1. Ecological investigation limits (EIL) are shown as vertical dashed lines where relevant.

4. Discussion

4.1 Concentrations of potential contaminants

Surface soils in the Charles Veryard and Smith’s Lake Reserves were largely uncontaminated with any of the elements measured. No potential contaminant in surface soil or subsoil exceeded any relevant human health guideline for recreational/public open space land use (Table 2). This may reflect rehabilitation of the site to parkland using techniques as simple as covering with clean fill, which is known to suppress the surface expression of soil contamination [38]. In surface soil, the only element to exceed a guideline value was Zn which had concentrations greater than the 200 mg/kg EIL threshold [37] in the southeast (2 samples) and northeast (1 sample) of Charles Veryard Reserve. More subsoil than surface soil samples exceeded EIL thresholds (Table 2)

The exceedance of EIL guideline values by Zn in a few surface soil samples and several subsoil samples in the eastern zones of Charles Veryard Reserve (Table 2, Figure 5, and Figure 11) reflects the common occurrence of zinc in urban environments, especially building materials and road traffic, and export of Zn into soil environments [39,40]. Very few toxicological studies exist on the effects of zinc on typical sports turf

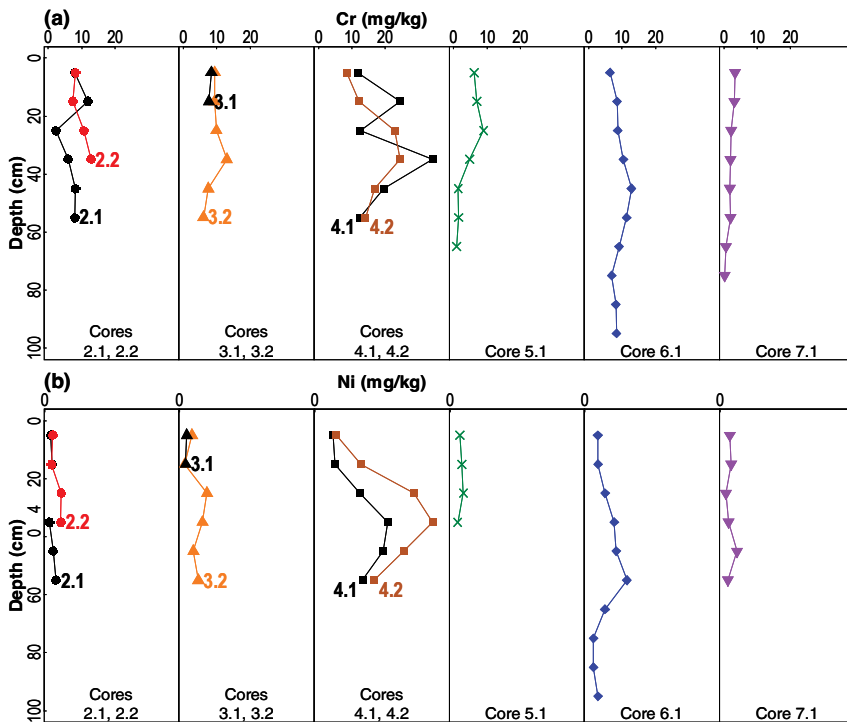


Figure 10. Depth profiles of (a) chromium (Cr) and (b) nickel (Ni) in soil cores collected from Smith's Lake and Charles Veryard Reserves, City of Vincent, Western Australia. Core locations from Figure 1.

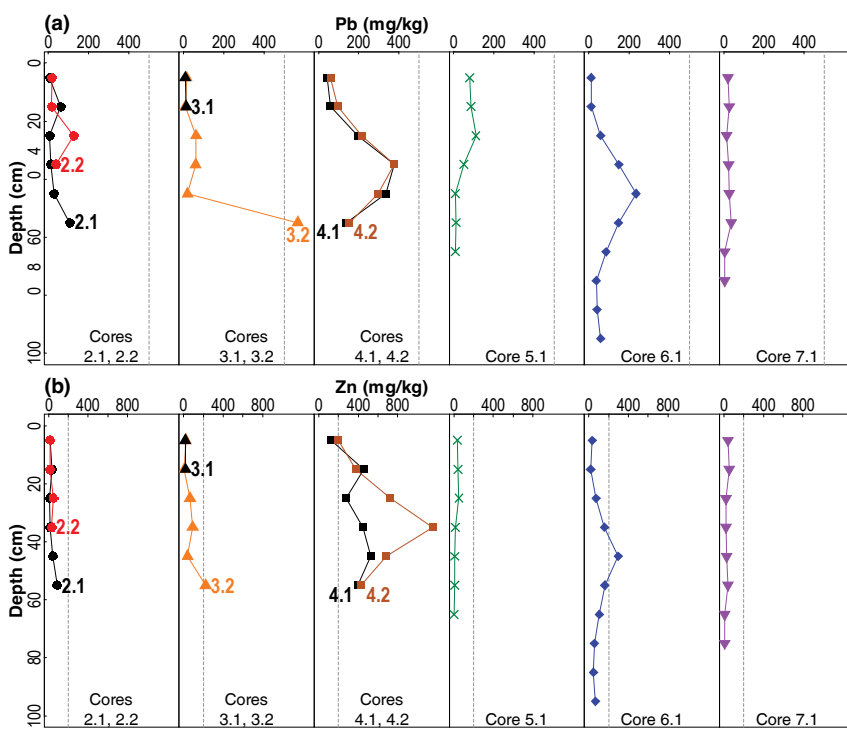


Figure 11. Depth profiles of (a) lead (Pb) and (b) zinc (Zn) in soil cores collected from Smith's Lake and Charles Veryard Reserves, City of Vincent, Western Australia. Core locations from Figure 1. Ecological investigation limits (EIL) are shown as vertical dashed lines where relevant.

plants or the microbial ecology in these environments; the likelihood that this Zn represents anthropogenic additions means that the bioavailability of Zn would therefore also be expected to be greater than for native soil Zn [36,41].

4.2 Spatial patterns of potential contaminants in surface soil

Although the incidence of actual surface soil contamination was low at Charles Veryard and Smith's Lake Reserves, the zone in which most enrichment of potential contaminants (As, Cr, Cu, Pb, and Zn) occurred coincided with the greatest subsoil concentrations of these elements (Figure 9, Figure 10, and Figure 11). This was the CVR-SE zone, in which the greatest number of point-variable combinations had significant high-high local Moran's I statistics (Table 3), confirming the visualizations generated by inverse-distance interpolation (Figure 3 to Figure 6). Based on these analyses, the south-east corner of Charles Veryard reserve, an area approximately 40 m N-S and 20 m E-W (ca. 800 m²), is contaminated with As, Cu, Pb, and Zn, a finding supported by the Integrated Pollution Index (Figure 6b). Based on a single sample with significant high-high Local Moran's I, and weak evidence of subsoil enrichment, Cr contamination may also be present in this location. However, the Global Moran's I statistics for Cr and Ni could not reject the null hypothesis of no spatial pattern, and no local Moran's I values were significant for Ni, so it is unlikely that either Cr or Ni have been added by contamination processes at the study site. Both Cr and Ni also had significant isolated high concentrations (significant high-low local Moran's I; Figure 4) which were not co-located; no isolated high concentrations were observed for As, Cu, Pb, or Zn.

The CVR-SE zone was the location of soil cores showing the greatest concentrations of As, Cr, Cu, Ni, and Zn, and the most exceedances of each element's ecological investigation limit (EIL) concentrations (Figure 9, Figure 10, Figure 11). Pb concentrations in subsoil at this location were also high, although

the greatest concentration occurred in Core 3.2 in the west of Charles Veryard Reserve. The co-location of surface soil contamination identified by spatial analysis with subsoil contaminant maxima confirms the south-east Charles Veryard Reserve area as the only location of significant contamination.

4.3 Associations of potential contaminants

Despite the minimal surface soil contamination, the identification of distinct soil zones based on their geochemical properties (Figure 3 and Figure 5) suggested that these different zones may represent the signatures of past activities or construction at the Charles Veryard and Smith's Lake Reserves. The element associations identified in the soil zones were supported by the Principal Components Analysis (Figure 7).

The associations identified by Principal Components Analysis are consistent, and also make geochemical sense. The nutrient elements K, P, and S probably represent a common source from historical horticulture [42]. The grouping of Ca, [Mg], Sr, and Ba includes elements which are all commonly associated with carbonates and/or cement-based materials [35]. The metal contaminants Cu, Zn, and Pb often have a common source such as building materials or roads and traffic [43]. Finally, Fe, As, Cr, and V reflect the commonly-observed associations of As, Cr, and V with iron oxides in soils [44], and Cr and V are used with Fe in manufacture of some steel products [45].

The association of Cu, Pb, and Zn in PC1-PC2 space, and to some extent As and Cr in the second principal component dimension, validated the calculation of the Integrated Pollution Index (IPI) from these elements. The IPI values are unusually high (range 6 – 28), reflecting the somewhat low values used for background concentrations. Reliable background concentrations for trace elements in soils of the Swan Coastal Plain around metropolitan Perth are still subject to

uncertainty, and obtaining these should be a priority for local research.

The low pH and low concentrations of many elements in the north-west of Charles Veryard Reserve most likely reflect a very sandy (*i.e.* poorly buffered) soil material which has been subject to minor acidification. This acidification may have originated from historical or recent disturbance of the underlying peaty acid sulfate soil material (*e.g.*, by light pylon installation), given the classification of much of the Charles Veryard and Smith's Lake Reserves area as being high to moderate risk of acid sulfate soil within 3 m of the land surface (Figure 1).

Elevated concentrations of Cu, Pb, and Zn in the north-east of Charles Veryard Reserve most likely represent contributions from construction (the Macedonian Centre, buildings on Albert Street) and possibly road traffic [39,46]. A road traffic origin for Pb is supported by the significant negative relationship of Pb with distance from roads (Figure 8). Construction and historical waste disposal sources are likely to have contributed Cu, and Pb to the south-east of Charles Veryard Reserve. The Charles Veryard Reserve south-east soil zone also has elevated pH, Al and Fe, however, so background concentrations may be naturally higher due to greater clay and/or iron oxide content of soils [44]. The greater concentrations of arsenic are most likely due to retention on Fe oxides, since there are no obvious sources of contamination and As concentrations are generally low. The greater concentrations of Al and Fe may themselves represent contamination from disposal of metalliferous wastes.

Soil in the south-west of Smith's Lake Reserve is characterized by higher pH and concentrations of Ca, Sr, Na, and P (and possibly K, S, and Mn). The high pH and elevated Ca and Sr are likely to represent additions of limestone or cement-based building materials [47]. Such additions are plausible given the relatively recent (2008) demolition of the Len Fletcher Sports Pavilion in the south of Smith's Lake Reserve. Enrichment

with the nutrient elements P, K, and S, and also Na, may reflect historical market gardening at the site and associated use of fertilisers, or organic amendments such as composts or manures [1].

The weak but significant trend in lead and vanadium concentrations as a function of distance from roads (Figure 8) suggests that road traffic was a significant source of these elements, in agreement with previous studies [48]. Since leaded fuels are no longer used in Australia and numerous other countries, the inputs of Pb are likely to represent a historical legacy of Pb accumulation in roadside soils. The abrasion of road surfaces by traffic is a potential source of vanadium from bituminous materials used as asphalt binders [49].

Concentrations of Cu, Pb, and Zn in soil profiles exceeded Ecological Investigation Limits (EILs) in several samples, especially for Zn (Figure 9, Figure 11). Most of these higher concentrations, however, were in deeper subsoil samples, so the risk to biota (mainly plant and microbial uptake) would therefore be expected to be minimal.

The existence of subsoil maximum concentrations at some locations may represent burial of waste material or drain sediment, or an evaporation/redox front resulting in accumulation of some elements. Given that that waste disposal at the Smith's Lake and Charles Veryard Reserves site is known to have been widespread [50,51], waste material would seem the most likely source. The relatively high subsoil concentrations of trace elements may represent a health risk, for example if dust is generated during excavation [52]. The potential risk should be considered in the context of a children's playground adjacent to the most contaminated surface soils and soil profiles.

Conclusions

An important conclusion from the initial concentration data is that the surface soil and subsoil sampled in this study at Smith's

Lake and Charles Veryard Reserves is not contaminated with As, Cr, Cu, Ni, Pb, or Zn from a human health perspective. There was, however, multiple exceedance of ecological investigation trigger limits (EIL) for Zn in surface soil and Cu, Pb, and Zn in subsoil. The spatial analysis showed that, on the basis of global and local Moran's I, distributions of most elements were not random but showed clustering. In line with the initial hypothesis, this significant clustering of adjacent higher concentrations in surface soil allowed identification of a specific area which, at the scale of sampling design, represented inputs from a point source of As, Cu, Pb, and Zn. At this site, the specific area of surface soil contamination was co-located with the most significant subsoil contamination, but this may not be a general result.

The combination of multivariate geochemical analysis with spatial information allowed both identification of realistic associations of elements, including potential contaminants. In particular, there was a consistent association of the dominant contaminants (Cu, Pb, and Zn) in the south-east of Charles Veryard Reserve which could be deduced from univariate spatial autocorrelation analysis, a composite contamination index (IPI), and multivariate principal components analysis.

In this study, the location and significance of potential contamination in the soil of urban public open space has been assessed thoroughly by measurement of multiple parameters, and rigorous spatial and statistical analysis. It is recommended that any such study uses a similar approach if soil contamination is suspected, especially given the global tendency for urban populations to increase and for redevelopment of, and increased population density in, inner-city precincts.

Supplementary Materials: The following are available online at <https://www.mdpi.com/article/10.3390/soilsystems5030046/s1>: Figure S1: 'Depth profiles of pH, EC, and Fe in soil cores collected from Smith's Lake and Charles Veryard Reserves, City of Vincent, Western Australia';

Table S1: 'Matrix of Spearman correlation coefficients for pH, EC, and elemental composition of soil samples from Smith's Lake and Charles Veryard Reserves. Values in bold type indicate a significant correlation ($p \leq 0.05$, using Holm's adjusted p-values for multiple comparisons)';

Table S2: 'Component Loadings for PC1-PC8';

Table S3: 'Summary of Principal Components';

Table S4: 'Eigenvalues (variances) for the first 8 components';

Funding: This research received no external funding.

Data Availability Statement: The raw data and metadata have been submitted to the PANGAEA repository at <https://doi.pangaea.de/10.1594/PANGAEA.935591>

Acknowledgments

The City of Vincent, Western Australia, granted permission to sample soil in the reserves. The principal investigator is extremely grateful to the ENVT3361 classes of 2017 and 2018 at The University of Western Australia, who did most of the work to generate the data: collecting samples, conducting the laboratory analyses, and uploading analytical results. Kirsty Brooks and Emielda Yusiharni from the School of Agriculture and Environment at The University of Western Australia made substantial efforts by managing the teaching laboratories, and organising field gear. Michael Smirk conducted the ICP-OES measurements.

Conflicts of Interest: The author declares no conflict of interest.

References

- Demiguel, E.; Degrado, M.J.; Llamas, J.F.; Martindorado, A.; Mazadiego, L.F. The overlooked contribution of compost application to the trace element load in the urban soil of Madrid (Spain). *Science of The Total Environment* **1998**, *215*, 113-122, doi:10.1016/S0048-9697(98)00112-0.

- Chen, T.B.; Wong, J.W.C.; Zhou, H.Y.; Wong, M.H. Assessment of trace metal distribution and contamination in surface soils of Hong Kong. *Environmental Pollution* **1997**, *96*, 61-68, doi:10.1016/S0269-7491(97)00003-1.
- Gaw, S.K.; Wilkins, A.L.; Kim, N.D.; Palmer, G.T.; Robinson, P. Trace element and ΣDDT concentrations in horticultural soils from the Tasman, Waikato and Auckland regions of New Zealand. *Science of The Total Environment* **2006**, *355*, 31-47, doi:10.1016/j.scitotenv.2005.02.020.
- Tarzia, M.; De Vivo, B.; Somma, R.; Ayuso, R.A.; McGill, R.A.R.; Parrish, R.R. Anthropogenic vs. natural pollution: An environmental study of an industrial site under remediation (Naples, Italy). *Geochemistry: Exploration, Environment, Analysis* **2002**, *2*, 45-56, doi:10.1144/1467-787302-006.
- Appleyard, S.; Wong, S.; Willis-Jones, B.; Angeloni, J.; Watkins, R. Groundwater acidification caused by urban development in Perth, Western Australia: Source, distribution, and implications for management. *Australian Journal Of Soil Research* **2004**, *42*, 579-585, doi:10.1071/SR03074.
- Orndorff, Z.W.; Daniels, W.L.; Fanning, D.S. Reclamation of acid sulfate soils using lime-stabilized biosolids. *Journal Of Environmental Quality* **2008**, *37*, 1447-1455, doi:10.2134/jeq2007.0206.
- Grundy, S.L.; Bright, D.A.; Dushenko, W.T.; Dodd, M.; Englander, S.; Johnston, K.; Pier, D.; Reimer, K.J. Dioxin and furan signatures in northern Canadian soils: Correlation to source signatures using multivariate unmixing techniques. *Chemosphere* **1997**, *34*, 1203-1219, doi:10.1016/s0045-6535(97)00419-0.
- Riemann, U. Impacts of urban growth on surface water and groundwater quality in the City of Dessau, Germany. In

- Impacts of Urban Growth on Surface Water and Groundwater Quality*, Ellis, B., Ed., IAHS-AISH Publication no. 259, International Association of Hydrological Sciences Press: Wallingford, UK, 1999; pp. 307-314.
9. Liu, E.; Yan, T.; Birch, G.; Zhu, Y. Pollution and health risk of potentially toxic metals in urban road dust in Nanjing, a megacity of China. *Science of The Total Environment* **2014**, 476-477, 522-531, doi:10.1016/j.scitotenv.2014.01.055.
 10. Henderson, F.M.; Xia, Z.G. SAR applications in human settlement detection, population estimation and urban land use pattern analysis: a status report. *IEEE Transactions on Geoscience and Remote Sensing* **1997**, 35, 79-85, doi:10.1109/36.551936.
 11. Huo, X.N.; Zhang, W.W.; Sun, D.F.; Li, H.; Zhou, L.D.; Li, B.G. Spatial pattern analysis of heavy metals in Beijing agricultural soils based on spatial autocorrelation statistics. *International Journal of Environmental Research and Public Health* **2011**, 8, 2074-2089, doi:10.3390/ijerph8062074.
 12. Anselin, L. Local Indicators of Spatial Association—LISA. *Geographical Analysis* **1995**, 27, 93-115, doi:10.1111/j.1538-4632.1995.tb00338.x.
 13. Hojati, S. Use of spatial statistics to identify hotspots of lead and copper in selected soils from north of Khuzestan Province, southwestern Iran. *Archives of Agronomy and Soil Science* **2019**, 65, 654-669, doi:10.1080/03650340.2018.1520977.
 14. Zhang, C.; Luo, L.; Xu, W.; Ledwith, V. Use of local Moran's I and GIS to identify pollution hotspots of Pb in urban soils of Galway, Ireland. *Science of the Total Environment* **2008**, 398, 212-221, doi:10.1016/j.scitotenv.2008.03.011.
 15. City of Vincent. *Thematic History*; City of Vincent: Leederville, Western Australia, 2008.
 16. Claise Brook Catchment Group. Restoration of Smith's Lake. Available online: http://www.cbeg.org.au/projects_smiths.html (accessed on 31.10.2017).
 17. Western Australian Land Information Authority. Landgate Map Viewer Plus. Available online: <https://maps.landgate.wa.gov.au/maps-landgate/registered/> accessed via <https://www0.landgate.wa.gov.au/maps-and-imagery/imagery/aerial-photography/aerial/> (accessed on 29 June 2021).
 18. Rayment, G.E.; Lyons, D.J. *Soil Chemical Methods - Australasia* CSIRO Publishing Clayton, Victoria, Australia, 2010.
 19. U.S. EPA. Method 3050B: Acid Digestion of Sediments, Sludges, and Soils *Test Methods for Evaluating Solid Waste, Physical/Chemical Methods, EPA publication SW-846 2007, Revision 6, February 2007*.
 20. Lynch, J. Additional provisional elemental values for LKSD-1, LKSD-2, LKSD-3, LKSD-4, STSD-1, STSD-2, STSD-3 and STSD-4. *Geostandards Newsletter* **1999**, 23, 251-260, doi:10.1111/j.1751-908X.1999.tb00577.x.
 21. Long, X.X.; Yang, X.E.; Ni, W.Z.; Ye, Z.Q.; He, Z.L.; Calvert, D.V.; Stoffella, J.P. Assessing zinc thresholds for phytotoxicity and potential dietary toxicity in selected vegetable crops. *Communications In Soil Science And Plant Analysis* **2003**, 34, 1421-1434, doi:10.1081/css-120020454.
 22. R Core Team. *R: A language and environment for statistical computing (Version 4.0.3)*; R Foundation for Statistical Computing: Vienna, Austria, <https://www.R-project.org>, 2020.
 23. Pohlert, T. *PMCMRplus: Calculate Pairwise Multiple Comparisons of Mean Rank Sums Extended (R Package)*, <http://CRAN.R-project.org/package=PMCMR>, 2018.
 24. eReimann, C.; Filzmoser, P.; Garrett, R.G.; Dutter, R. *Statistical Data Analysis Explained: Applied Environmental Statistics with R*, First ed.; John Wiley & Sons: Chichester, England, 2008; p. 343.
 25. Fellows, I. *OpenStreetMap: Access to open street map raster images, using the JMapView library by Jan Peter Stotz*, 0.3.3; (R Package Version 0.3.4) <http://CRAN.R-project.org/package=OpenStreetMap>, 2019.
 26. Google. Getting Started | Google Maps Elevation API | Google Developers. Available online: <https://developers.google.com/maps/documentation/elevation> (accessed on 09/10/2017).
 27. Cooley, D. *googleway: Accesses Google Maps APIs to Retrieve Data and Plot Maps. R package version 2.0.0*, 2017.
 28. Akima, H.; (FORTRAN code); Gebhardt A. (port); Petzoldt T. (aspline function); Maechler M. (interp2xyz; enhancements and corrections) *akima: Interpolation of irregularly spaced data. R package version 0.5-11*. <http://CRAN.R-project.org/package=akima>, 2013.
 29. Kalogirou, S. *lctools: Local Correlation, Spatial Inequalities, Geographically Weighted Regression and Other Tools. R package version 0.2-8*. Available online: <https://CRAN.R-project.org/package=lctools> (accessed on 28 May 2021).
 30. Pebesma, E.; Bivand, R. *sp: Classes and Methods for Spatial Data. R package version 1.4-4*, 2020.
 31. Pebesma, E.J.; Graeler, B. *gstat: Spatial and Spatio-Temporal Geostatistical Modelling, Prediction and Simulation. R package version 2.0-7*, 2021.
 32. Webster, R.; Oliver, M.A. How large a sample is needed to estimate the regional variogram adequately? *Geostatistics Troia '92. Vol. 1* **1993**, 155-166.

33. Sun, Y.; Zhou, Q.; Xie, X.; Liu, R. Spatial, sources and risk assessment of heavy metal contamination of urban soils in typical regions of Shenyang, China. *Journal of Hazardous Materials* **2010**, *174*, 455-462, doi:10.1016/j.jhazmat.2009.09.074.
34. DWER. *Final report: Review of the uncontaminated fill thresholds in Table 6 of the Landfill Waste Classification and Waste Definitions 1996 (as amended 2018)*; Department of Water and Environmental Regulation, Government of Western Australia: Joondalup, Western Australia, December 2019 2019.
35. Rate, A.W. Multielement geochemistry identifies the spatial pattern of soil and sediment contamination in an urban parkland, Western Australia. *Science of The Total Environment* **2018**, *627*, 1106-1120, doi:10.1016/j.scitotenv.2018.01.332.
36. National Environment Protection Council. Schedule B (1): Guideline on the Investigation Levels for Soil and Groundwater. In *National Environment Protection (Assessment of Site Contamination) Measure (Amended)*; Commonwealth of Australia: Canberra, 2013.
37. National Environment Protection Council. Schedule B (1): Guideline on the Investigation Levels for Soil and Groundwater. In *National Environment Protection (Assessment of Site Contamination) Measure*; Commonwealth of Australia: Canberra, 1999.
38. Rimmer, D.L.; Younger, A. Land Reclamation after Coal-mining Operations. In *Contaminated Land and its Reclamation*, Hester, R.E., Harrison, R.M., Eds.; Royal Society of Chemistry: Cambridge, UK, 1997; pp. 73-90.
39. Callender, E.; Rice, K.C. The urban environmental gradient: Anthropogenic influences on the spatial and temporal distributions of lead and zinc in sediments. *Environmental Science and Technology* **2000**, *34*, 232-238, doi:10.1021/es990380s.
40. Charlesworth, S.; de Miguel, E.; Ordóñez, A. A review of the distribution of particulate trace elements in urban terrestrial environments and its application to considerations of risk. *Environmental Geochemistry and Health* **2011**, *33*, 103-123, doi:10.1007/s10653-010-9325-7.
41. Smolders, E.; Oorts, K.; van Sprang, P.; Schoeters, I.; Janssen, C.R.; McGrath, S.P.; McLaughlin, M.J. Toxicity of trace metals in soil as affected by soil type and aging after contamination: using calibrated bioavailability models to set ecological soil standards. *Environmental Toxicology and Chemistry* **2009**, *28*, 1633-1642, doi:10.1897/08-592.1.
42. Pietrzak, U.; McPhail, D.C. Copper accumulation, distribution and fractionation in vineyard soils of Victoria, Australia. *Geoderma* **2004**, *122*, 151-166, doi:10.1016/j.geoderma.2004.01.005.
43. Harrison, R.M.; Laxen, D.P.H.; Wilson, S.J. Chemical associations of lead, cadmium, copper, and zinc in street dusts and roadside soils. *Environmental Science and Technology* **1981**, *15*, 1378-1383, doi:10.1021/es00093a013.
44. Hamon, R.E.; McLaughlin, M.J.; Gilkes, R.J.; Rate, A.W.; Zarcinas, B.; Robertson, A.; Cozens, G.; Radford, N.; Bettenay, L. Geochemical indices allow estimation of heavy metal background concentrations in soils. *Global Biogeochemical Cycles* **2004**, *18*, doi:10.1029/2003GB002063.
45. Tanner, P.A.; Ma, H.L.; Yu, P.K.N. Fingerprinting metals in urban street dust of Beijing, Shanghai, and Hong Kong. *Environmental Science and Technology* **2008**, *42*, 7111-7117, doi:10.1021/es8007613.
46. Davis, A.P.; Shokouhian, M.; Ni, S. Loading estimates of lead, copper, cadmium, and zinc in urban runoff from specific sources. *Chemosphere* **2001**, *44*, 997-1009, doi:10.1016/S0045-6535(00)00561-0.
47. Jim, C.Y. Urban soil characteristics and limitations for landscape planting in Hong Kong. *Landscape and Urban Planning* **1998**, *40*, 235-249, doi:10.1016/S0169-2046(97)00117-5.
48. Mielke, H.W.; Laidlaw, M.A.S.; Gonzales, C. Lead (Pb) legacy from vehicle traffic in eight California urbanized areas: Continuing influence of lead dust on children's health. *Science of The Total Environment* **2010**, *408*, 3965-3975, doi:10.1016/j.scitotenv.2010.05.017.
49. Béze, L.E.; Rose, J.; Mouillet, V.; Farcas, F.; Masion, A.; Chaurand, P.; Bottero, J.-Y. Location and evolution of the speciation of vanadium in bitumen and model of reclaimed bituminous mixes during ageing: Can vanadium serve as a tracer of the aged and fresh parts of the reclaimed asphalt pavement mixture? *Fuel* **2012**, *102*, 423-430, doi:10.1016/j.fuel.2012.06.080.
50. Conacher, J. *Historic Land Use Survey of the Claisebrook Catchment*; The University of Western Australia for the Claisebrook Catchment Group: 2000; p. 61.
51. City of Vincent. Charles Veryard Reserve, Place Number 17957. In *inHerit - Places Database*, Heritage Council of WA, Ed.; Perth, Western Australia, 2007.
52. Ljung, K.; Maley, F.; Cook, A. Canal estate development in an acid sulfate soil-Implications for human metal exposure. *Landscape and Urban Planning* **2010**, *97*, 123-131, doi:10.1016/j.landurbplan.2010.05.003.

The paper first published in Soil Syst. 2021, 5, 46. <https://doi.org/10.3390/soilsystems5030046> is republished with authors' consent.

Copyright: © 2021 by the authors. Submitted for possible open access publication under the terms and conditions of the Creative Commons Attribution (CC BY) license (<https://creativecommons.org/licenses/by/4.0/>). 

Mapping physical development changes using Geospatial techniques

The aim of this research is to produce a new and updated map Lagos Island Local Government Area, Nigeria and document changes that have occurred over time

Leonard Michael Onyinyechi Aminigbo
 Department of Geography and
 Environmental Management, Rivers State
 University, Portharcourt, Nigeria

Abstract

The scope of the research work comprised the planning and preliminary data requirement analyses, acquisition of preliminary data such as base map, data processing and database creation process, GIS implementation using linear referencing, map creation and analyses of data as well as the presentation of results. The aim of this research is to produce a new and updated map of the study area and document changes that have occurred over time. The objectives therefore includes; obtaining an older map of Lagos Island and update its features, obtaining the GPS coordinates within the study area for geo-referencing, analyzing the land use patterns for the study area, producing a new map in a Geospatial Information System Environment and analyzing the social-economic activities within the study area. The study area of this research is *Lagos Island Local Government Area*, in Lagos State, Nigeria. It is located in the South-western part of Lagos. The Study area is Located to the extreme south of Lagos, within the latitude 6°22'- 6°25'N and Longitude 3°25'E around Atlas Cove Depot and Jetty. Methodologically, this study employed field studies where equipments such as Garmin GPS MAP 62 (Series), Data storage, manipulation and retrieval hardwares were deployed. GIS operations were carried out using softwares such ArcGIS 10.8, AutoCAD 2007 for drafting, GoogleEarth-4.2 pro Application, Microsoft Excel 2007 for the storage of easting and northing (x, y) values, for all segment points and points

of interest in the study area ArcGIS 10.8 software was used for Dynamic segmentation process and GIS analysis involving spatial analysis and search while Microsoft Word 2007 was used for documentation. The result showed new spatial features such as reclaimed wet lands, new roads, buildings and social amenities located in the updated map. Finally the study by demonstrating the capacity of the use GIS and remote sensing techniques for updating of maps.

Introduction

Maps have being used for centuries to represent the environment, and shows locations, distances, directions as well as size of an area or region. Maps also display geographic relationships, differences, clusters and patterns. It can further be explore for other purposes such as navigation, exploration, and illustration. More so, for identification of infrastructural positions and their availabilities, even for communication of activities such as resource, disaster [6].

Mapping has been an integral part of census taking for a long time. Very few enumerations during the last several census rounds were executed without the help of detailed maps. In general terms, digital mapping serves several purposes in policy decisions as well as implementation. Cartography has been affected by the information revolution somewhat later than other fields. Early computers were good at storing numbers

and text [12]. Maps, in contrast, are complex, and digital mapping requires large data storage capacity and fast computing resources. Furthermore, mapping is fundamentally a graphical application, and early computers had limited graphical output capabilities [13]. The earliest mapping applications implemented on computers in the 1960s did not therefore find wide application beyond a few government and academic projects. It took until the 1980s for commercial geographic information systems to reach a level of capability of getting it right. GIS facility now plays a key role in helping to make map making easier in computerised environment. It is an application designed for geo-data base data collection, manipulation and graphical expression [8, 16].

2. GIS applications

Digital mapping and spatial analyses have been developed simultaneously in several related fields. The present status would not have been achieved without close interaction between various fields such as utility networks, cadastral mapping, topographic mapping, thematic cartography, surveying and photogrammetry, remote sensing, image processing, computer science, rural and urban planning, earth science and geography. The GIS technology is rapidly becoming a standard tool for management of natural resources. The effective use of large spatial data volumes is dependent upon the existence of an efficient geographic handling and processing system to transform this data into usable information.

The GIS technology is used to assist decision-makers by indicating various alternatives in development and conservation planning and by modelling the potential outcomes of a series of scenarios. It should be noted that any task begins and ends with the real world. Data collected are about the real world. Of necessity, the product is an abstraction; it is not possible (and not desired) to handle every detail. After the analyses of data,

information is compiled for decision-makers. Based on this information compiled, actions area taken and plans implemented in the real world. This is what the GIS technology has helped in doing and more fields are beginning to see the necessity of the Geographic Information System (GIS) [12].

2.1. Major areas of application of GIS

Some of the major areas of the application of GIS are briefly described below.

1. Street Network Based Application - It is an addressed matched application, vehicle routing and scheduling location and site selection and disaster planning.
2. Different streams of planning - Such as urban planning, housing, transportation planning architectural conservation, urban design, and landscape.
3. Natural Resource Based Application - Management and environmental impact analysis of wild and scenic recreational resources, flood plain, wetlands, aquifers, forests, and wildlife.
4. View Shed Analysis - Hazardous or toxic factories siting and ground water modelling. Wild life habitat study and migration route planning.
5. Land Parcel Based - Zoning, subdivision plans review, land acquisition, environment impact analysis, boundary justification, nature quality management and maintenance etc.
6. Facilities Management - GIS can help in the location of underground pipes and cables for maintenance, planning, tracking, energy use.

2.2. Scope of the study

The scope of the research work is as follows;

1. Planning and preliminary data requirements analyses.
2. Acquisition of preliminary data, like Base Map.
3. Data processing and database creation process.
4. GIS implementation using linear referencing.
5. Map creation and Analyses of data.
6. Analyses and Presentation of results.

2.3. Aim and objectives

The aim of this research is to produce a new and updated map of the study area and document changes that have occurred over time.

The objectives of the project are as follows:

1. To obtain an older map of Lagos Island and update its features.
2. Obtain the GPS coordinates within the study area for geo-referencing.
3. To Analyse the land use patterns for the study area.
4. To produce a new map in a Geospatial Information System Environment.
5. To analyze the social-economic activities within the study area.

2.4. The study area

The study area of this research is *Lagos Island Local Government Area*, in Lagos State, Nigeria. It is located in the South-western part of Lagos. The Study area is Located to the extreme south of Lagos, within the latitude 6°22'- 6°25'N and Longitude 3°25'E around Atlas Cove Depot and Jetty. Atlas Cove is located at the entrance of the Lagos Harbour (Commodore Channel) – the only main entrance of the Lagos Lagoon and Badagry Creek complex to the Atlantic Ocean and directly opposite the East Mole, Some 2.5km south of the Apapa port complex and about 1.75km north of the Lighthouse Beach (takwa Bay Beach). Administratively, It shares its northern boundary with Lagos Mainland LGA and the Lagos lagoon, to the east it is bounded by Eti – Osa L.G.A. and to the west by Apapa L.G.A. It covers an area of 4.993 Sq. Kilometres (figure 1). The area is low lying with an elevation of about 0.5-3m above sea level [3].

Lagos Island is connected to the mainland by three large bridges which cross Lagos Lagoon to the district of Ebute Metta. It is also linked to the neighbouring island of Ikoyi and to Victoria Island. The Lagos harbour district of Apapa faces the western side of the island. Forming the main commercial district of Lagos, Lagos

Island plays host to the main government buildings, shops and offices. The Catholic and Anglican Cathedrals as well as the Central Mosque are located here.

The study area falls within the hot humid equatorial climate that is generally experienced in the Lagos area with generally high temperature, humidity and rainfall. The mean annual temperature for the area is about 27.5°C. The mean monthly minimum temperature is about 24°C and the mean monthly maximum temperature is about 29.5°C. Lagos area receives an annual rainfall of about 1,524mm to 2,032mm with an annual mean of 1,800mm. The number of

rainy days is about 121 days. Although rainfall occurs all year round, it is not uniformly temporally distributed.

2.5. Significance of the research

This research is designed to equip scholars with the nitigrities of map making and interpretation as well as analysis of the spatial features of the map [4]. The data gathering of of spatial and non-spatial data features within the study area such as roads, rivers, railways, buildings etc, for effective interpretation of the map is a vital part of the whole exercise [15]. It will also help the student to be more familiar with the

GIS environment, with basic training on the easy logic to query and analyses features on a map. On the overall view, this research is significant in order to aid the student in the following areas: 1)

1. To enhance the student ability in map production.
2. To aid the student knowledge on the use of geospatial software.
3. To help the student analyse and interpret the features on the map.

2.6. Map update in the GIS enviroment

Digital map data are necessary for the achievement of producing a recent map in a ArcGis environment. One must have a prior knowledge about the area of concentration on available as a base map. (figure 1) We will use the term layers from this point on, since this is the recognized term used in ArcGIS. Layers represent, in a special digital storage format, features on, above, or below the surface of the earth. Depending on the type of features they represent, and the purpose to which the data will be applied, layers can be either a Vector data, which represent features as discrete points, lines, and polygons or a Raster data, which represent the landscape as a rectangular matrix of square cells. Hence, spatial data are often referred to as layers or coverage.



Source: Office of the surveyor General, Lagos state.
Figure 1. A base Map Lagos Island Area of Lagos State



Figure 2. Part of Lagos State Map showing the position of Lagos Island.

3. Materials and methods

This aspect centres on the steps involved in carrying out the project. It gives in details the breakdown of the tasks carried out to achieve the aim of the project [2, 11]. The description is as follows.

3.1. Project planning (reconnaissance)

Reconnaissance is the preparatory stage for project execution. It involves the overall assembling, examination, and collection or over viewing of project site or the study area and logistics for successful execution, that is, a successful project depends on a

good reconnaissance or preliminary investigation and planning exercise. Its value prior to the real survey work cannot be underestimated and it enables one to obtain the picture of the whole area in his mind to work economically in terms of time, labour, energy and funding [17].

For the purpose of the work, a precise reconnaissance was carried out on the study area in to have a grounded knowledge of the area in question.

The reconnaissance was carried out in two forms and they are as follows;

1. Planning
2. Field Reconnaissance.

3.1.1. Planning

The planning involved the collection of information about the study area, the necessary materials and equipments needed to carry out the project. It centred on the assembling of existing data, determining how to get to the study area as well as the needs analyses of the project. A careful understanding of the needs and the data to be obtained from the study area was well analysed.

3.1.2. Field reconnaissance

Field reconnaissance involves the actual visitation to the study area with the aim of determining the typical areas of interest and the existing features present in the study area. This visitation also help in knowing the best times to carry out the observations or data acquisition in order to obtain the best results at minimal cost. A preliminary detailed field study was carried out before the actual data acquisition process.

In essence, it requires a rigorous and strategic plan to be able to cover the numerous streets in few days to collect different sets of data, even with little available time. The team had to employ careful and intelligent strategy to achieve tangible result [1, 16].

(i) Systems Selection

This comprises of both the equipment and software used in the project execution. It includes the hardware and software used for data acquisition, management and information presentations.

(ii) Equipment

The equipments are as follows.

1. Garmin GPS MAP 62 (Series).
2. Data storage, manipulation and retrieval hardware: A host laptop computer with configuration Core 2 Duo, 250 Giga byte hard disk (memory space), 4GB of RAM.

(iii) Software

The software performs the GIS operations. The project was carried using the following software:

1. Window 7 was used Operating system was used for this project.
2. AutoCAD 2007 for drafting.
3. GoogleEarth-4.2 pro Application.
4. Microsoft Excel 2007 for the storage of easting and northing (x, y) values, for all segment points and points of interest in the study area.

5. ArcGIS 10.1 software was used for Dynamic segmentation process and GIS analysis involving spatial analysis and search.
6. Microsoft Word 2007 for documentation.

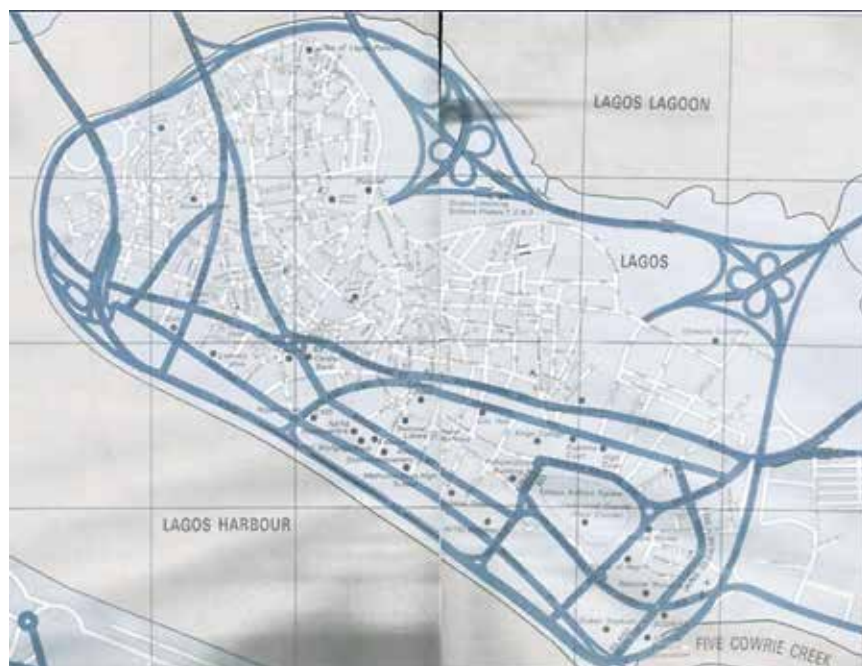
3.2. Preliminary data acquisition and operations

In the cause of the data acquisition process, we considered the requirements of the project in terms of its scope, objectives and of course the aim. Hence, after the planning stage, we resolved that the following preliminary data would be acquired.

1. A base map of the study area, showing the roads in the study area.
2. Coordinates of some points of interest for georeferencing of the base map.

These set of data were obtained and used to reproduce the map of the study area. This was of great importance as it prepared us for the actual fieldwork [14].

The map which served as a guide during the actual field operations was very handy and useful for easy



Source: Office of the surveyor General, Lagos state.

Figure 3. A base map of the study area (Lagos Island).

navigation on the best positions for the data acquisition process for the roads covered in Lagos Island Local Government Area.

3.3. Field operations

This aspect of the research is centred on the activities carried out on the field or study area. The fieldwork was in stages and at different days of the week. Roads to be covered were grouped and a particular day was attached. The description of fieldwork is as detailed in table 1.

Table 1. Field Activity Schedule.

S/n	Activities	Days Assigned
1	Determination of boundary	Day 1
2	Coordination of some points of interest in the study area	Day 2
3	Acquisition of Land use information for the Local Government Area	Day 3
4	Acquisition of non-spatial data in the area	Day 3

3.4. The recent status of the study area from a satellite view

Lagos Island has gone through a systematic metamorphous change simply due to the introduction of a reclamations project

just at the outer North-western part of the island. The new land project was completed around 2012, owned by the Lagos State

Government to introduce new type of development which is necessary for the demand for development, as a strategy to overcome the scare availability of empty vast land to suit recent building designs for both housing and commercial activities.

Figure 4 and figure 5 are the images of the new land name Ilubirin Housing Project.

4. Results

Below are the steps taken when carrying out the updated map of Lagos Island LGA Points of interest like Schools, Police stations, Churches, Mosques and other land use points were picked using the handheld GPS.

Steps taking:

1. Import the Base Map into AutoCAD Platform knowing the coordinate of major spots of on the map.
2. Geo-reference the points to related to the proper locations of the base to the earth surface.

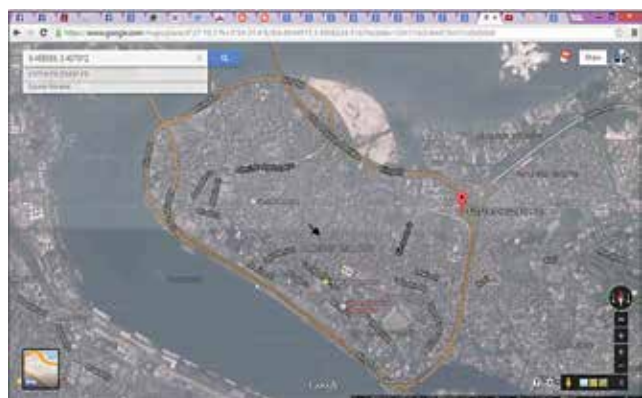


Figure 4. A view of the Ilubirin (Lagos Island) Reclamation, proposed for Housing Scheme Close to the Lagoon of Lagos.

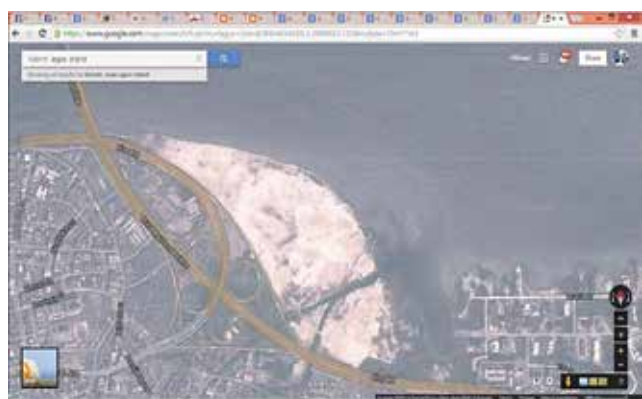


Figure 5. A closer resolution view of the Ilubirin (Lagos Island) Reclamation, proposed for Housing Scheme Close to the Lagoon of Lagos.

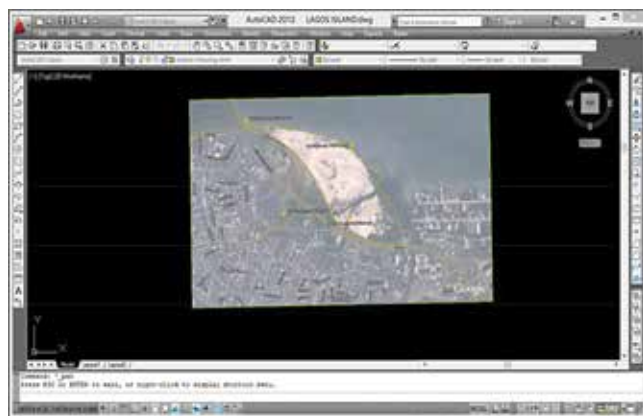


Figure 6. A print-screen of the digitize process in AutoCAD environment.



Figure 7. AutoCAD view of the reclaimed wetlands.

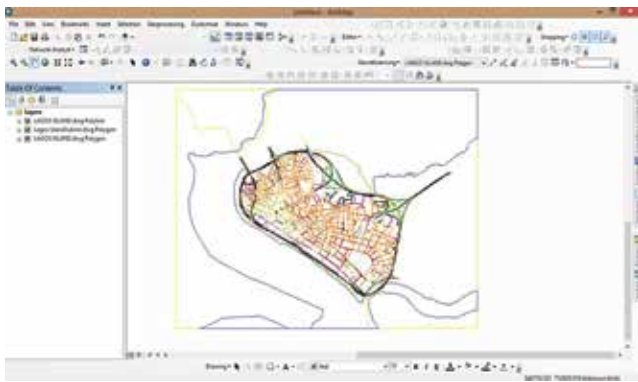


Figure 8. A printed screen of the map in ArcGIS environment.

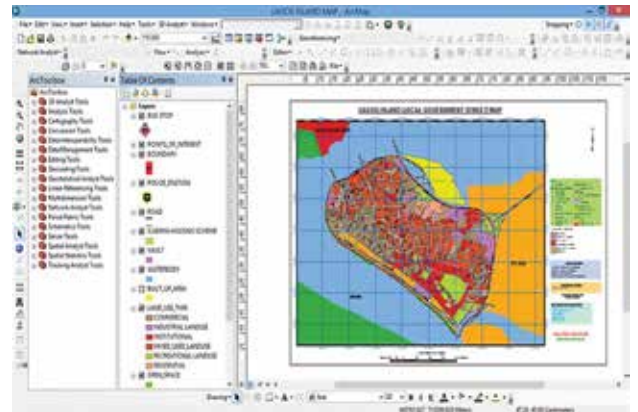


Figure 12. A printed screen of the map in ArcGIS environment.

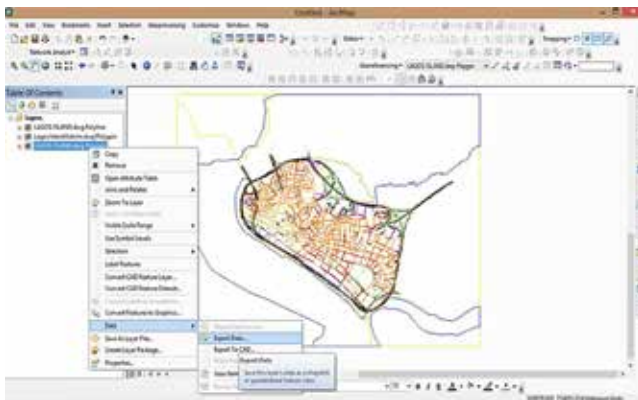


Figure 9. A printed screen of the map in ArcGIS environment.

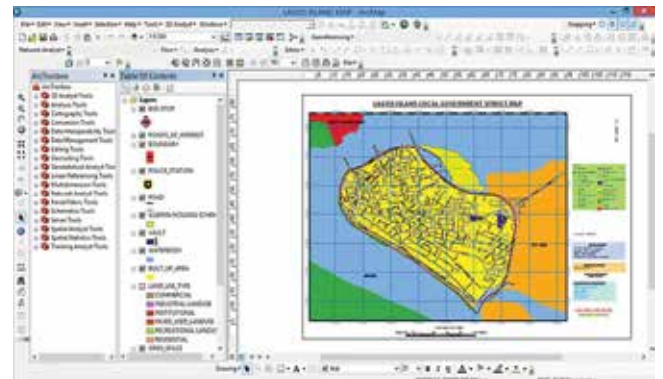


Figure 13. Final printed screen of the map in ArcGIS environment

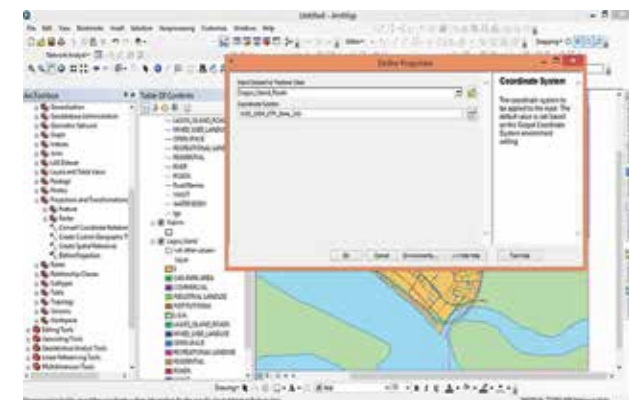


Figure 10. A printed screen of the map in ArcGIS environment.

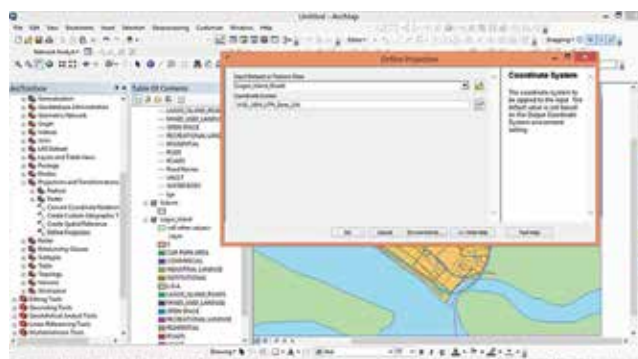


Figure 11. A printed screen of the map in ArcGIS environment.

3. Create layer for different properties that will be vectorized upon the base map.
4. Import the image of the new area Ilubirin (aerial view) and repeat step 1, 2, 3.
5. Vectorise the area with new layer- it suggested to name the layer (Ilubirin, as done in this exercise).
6. We imported all the vectors to ArcGIS environment.
7. Convert all Layers imported to Shape files (.shp) referencing it to the WGS 1984. Zone 31N Datum.
8. The shapefile (polygons, Polylines and Points) are modified with colour interpretation.
9. The last modification was done with layout view. This is where symbolic description, Title, Legends, Calibrations and North Symbol are inserted to produce a final map.

5. Conclusion

Lagos Island Local Government Area can be described as a place with a mixture of land use. It is referred to this because it comprises of commercial, institutional residential land uses [5]. This makes it a typical place for study, as the routes in the area are well affected by the various activities there in [6, 10]. The area is known for its robust commercial activities, by the present of huge market system, banking activities, and government institutional offices which give it an attraction to millions of

inhabitants daily to transact business. The advantage contributes thus as a factor to increasing population and development projects for housing and business [7, 9].

Furthermore, Lagos Island contains a central business district. This district is characterized by high-rise buildings. Other important activities and historical monuments in Lagos island are the locations of many of the city's largest wholesale marketplaces (such as the popular Idumota and Balogun markets), the National Museum of Nigeria, the Central Mosque, the Glover Memorial Hall, Christ's Church Cathedral (CMS) and the Oba Palace. Though formerly in a derelict condition, Lagos Island's Tinubu Square is a site of historical importance; it was here that the Amalgamation Ceremony that unified the North and South protectorate to form Nigeria took place in 1914.

One of the predominant problems facing Lagos metropolis is that of promoting development, which adversely leads to attraction of more populace, a causative to traffic congestion. This arises from the fact that Lagos metropolitan lands are becoming increasingly scarce resources. The point is that metropolitan Lagos requires land for numerous activities. On the other hand, land is a finite resource, while the demand for land increases, thereby posing challenges. It should be noted that human needs must be satisfied on the fixed land and development must be located on the limited land. Activities have to compete for the use of best sites for their location; hence the principle of optimality has to be adhered to at the expense of the specified space standards and permissible development in that location. Aluko, Ola (2011).

References

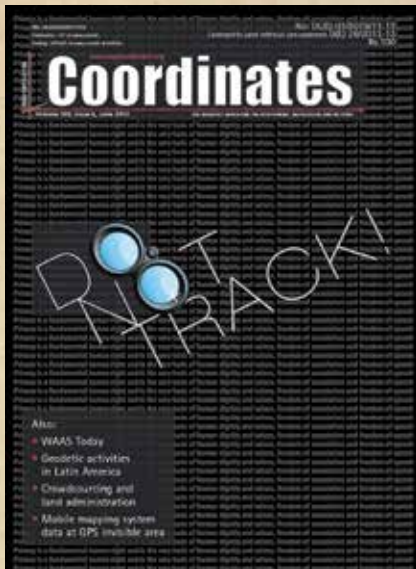
- [1] Adams, T. M., N. A. Koncz, et al., 2001. Guidelines for the implementation of multimodal transportation location referencing systems. Washington, DC, National Academy Press.
- [2] Amiegebor, D. 2007. Road Transport Network Analysis in Port Harcourt Metropolis, *Journal of Research in National Development* 51: 42-50.
- [3] Aminigbo, L. M. O et al (2021), Analyses of land use change in Etiosa L.G.A of Lagos State Nigeria from 2004 to 2010. *American Journal of Environmental Sciences and Engineering, USA*.
- [4] Binns, Sir Bernard O. (1953). Cadastral surveys and records of rights in land. Rome: FOA Land Tenure Study.
- [5] Briggs, D. W. and B. V. Chatfield 1987. "Integrated Highway Information Systems," NCHRP.
- [6] Burroughs, P. A. (1986). Principles of Geographical Information Systems. Principles and Applications. London: Longman.
- [7] Dale, P. F. and John D. McLaughlin (1989). Land Information Management. New York: Oxford University Press.
- [8] Dueker, K. J. 1987. Geographic Information Systems and Computer-Aided Mapping, "Journal of the American Planning Association". ESRI, 1993. User's Guide of Dynamic Segmentation, Redland, CA.
- [9] ESRI White Paper (2001). Organizational Structure for Local Government GIS. A survey: <http://www.esri.com>.
- [10] Fletcher, D. 1987. Modeling GIS Transportation Networks, "URISA Proceedings", Vol. II, pp. 84-92.
- [11] Goodchild, M. F., 2000. GIS and Transportation: Status and Challenges. *GeoInformatica*, 42, pp. 127-139.
- [12] Huang, B., 2003. An object model with parametric polymorphism for dynamic segmentation. *International Journal of Geographical Information Science*, 174, pp. 343-360.
- [13] Kansky, K. 1963. Structure of Transportation Network: Relationships between Network Geometry and Regional Characteristics, Research Paper 84. Chicago: University of Chicago. 155.
- [14] Li, X. and H. Lin, 2006. A Trajectory-Oriented, Carriageway Based Road Network Data Model, Part 2: Methodology *Geospatial Information Science*, 92, pp. 112-117.
- [15] Malaikrisanachalee, S. and T. M. Adams, 2005. Lane-based Network for Transportation Network Flow Analysis and Inventory Management. Transportation Research Board, 1935, pp. 101-110.
- [16] Miller, H. J.; Shaw, S. L. 2001. Geographic Information Systems for Transportation: Principles and Applications. New York: Oxford University Press. 470 p.
- [17] Obafemi A. A. et al. 2011. Road Network Assessment in Trans-Amadi, Port Harcourt in Nigeria Using GIS, *International Journal for Traffic and Transport Engineering*, 2011, 14: 257-264.

The paper originally published in American Journal of Environmental Science and Engineering. Volume 5, Issue 4, December 2021, pp. 113-123. doi: 10.11648/j.ajese.20210504.15 is republished with the authors' consent.

Copyright © 2021 Authors retain the copyright of this article. This article is an open access article distributed under the Creative Commons Attribution License (<http://creativecommons.org/licenses/by/4.0/>) which permits unrestricted use, distribution, and reproduction in any medium, provided the original work is properly cited. 

In Coordinates

10 years before...



mycoordinates.org/vol-8-issue-6-June-2012

Accuracy maintenance method for mobile mapping system data at GPS invisible area

Akihisa Imanishi, Kikuo Tachibana and Koichi Tsukahara
PASCO CORP, Japan

In this paper, accuracy investigation of Land Mark Update (LMU) which corrects MMS vehicle position utilizing ground control point was carried out and depending on this result development of accuracy maintenance method in GPS invisible area was considered.

Do Not Track!

George Cho

Institute for Applied Ecology and
Faculty of Applied Science
University of Canberra, Canberra, Australia

One wonders now whether geospatial technologies have exposed privacy, and whether this exposure has given rise to an unrealistic expectation of privacy protection. It may be that privacy has been poorly understood – involving emotional and mass fear and uncertainty so that calm reaction and contemplation has not taken place. In the Web 2.0 generation, where things happen by mass action, the solutions are embedded in technical and social standards and not solely in legal avenues.

WAAS Today

Deborah Lawrence

Federal Aviation Administration
Wide Area Augmentation System
(WAAS) Program Manager

Beyond continued system development, sustainment, and technology refresh activities for WAAS; future WAAS initiatives include support of global interoperable SBAS services including the development of SBAS in South America, dual-frequency multi-constellation (DFMC) SBAS, and Advanced Receiver Autonomous Integrity Monitoring (ARAIM).

Crowdsourcing and land administration

Robin McLaren

Director, Know Edge Ltd

Mobile phone and personal positioning technologies, satellite imagery, the open data movement, web mapping and wikis are all converging to provide the 'perfect storm' of change for land professionals. The challenge for land professionals is not just to replicate elements of their current services using crowdsourcing, but to radically rethink how land administration services are managed and delivered in partnership with citizens. Land administration by the people for the people can become a distinctly 21st century phenomenon.

Forest Survey of India says forest cover estimate is done with field data tallied with Satellite-based Interpretation

Amid criticism from experts of its methodology to map forest cover in the country, the Forest Survey of India (FSI) has said that the forest cover is estimated from the field inventory data, which corroborate the figures obtained from satellite-based interpretation. It claimed that the criticism of its findings was based on perception and done more to generate sensation.

Sticking to its assessment which shows how both forest and tree cover increased in India in the past two years, taking the total green cover to nearly one-fourth of the country's geographical area (GA) in 2021, the FSI has elaborated on how it did its biennial survey, based on globally-accepted standards, which was backed by an elaborate ground-truthing exercise.

FSI's 'India State of Forest Report (ISFR), 2021' was released by Environment minister Bhupender Yadav, which shows that 'forests' and 'trees outside recorded forest areas', put together, reported an increase of 2,261 sq km (0.3%) last year compared to the previous assessment in 2019. The increase took the overall green cover to 8,09,537 sq km (24.6% of GA) which includes 7,13,789 sq km of forest cover (21.7% of GA).

Critics, however, questioned the FSI's claim with one of them, M D Madhusudan, ecologist and co-founder of the Nature Conservation Foundation, even highlighting that the purported gains come largely from FSI's "problematic and perverse redefinition of 'forest' to include tea gardens, coconut plantations, urban built-up areas, native grasslands wrecked by invasive trees, and even treeless desert scrub". In his social media post, he said, "There is little evidence to show that India's

natural forest cover has actually increased. In fact, it has very likely declined."

Calling such remarks "factually incorrect", the FSI said it carried out an inventory of forest and trees outside forest on adequate sample points spread over the entire country. "The forest cover is also estimated from the field inventory data which corroborate the figures of forest cover obtained from satellite-based interpretation. Change polygons are ground-truthed by FSI as well as state governments, then only is the interpretation accepted," it said.

The FSI emphasised that it carries out "wall to wall forest cover mapping of the country", using remote sensing based methodology at two year intervals, and noted that the points raised by the critics were their "perception".

On critics' point on counting of tea gardens and coconut plantations as forest, the FSI flagged the definition of 'forest cover', used in the ISFR, where it is defined as "all lands, more than one hectare in area, with a tree canopy density of more than 10% irrespective of ownership and legal status. Such lands may not necessarily be a recorded forest area. It also includes orchards, bamboo, palm etc."

Referring to this globally accepted definition, the FSI said, "Those areas of tea gardens, which satisfy the above conditions and are captured by the satellite sensor are treated as forest cover, mainly due to the tree cover existing there. Depending upon the canopy density, they are categorised as 'open forest', 'moderately dense forest' and 'very dense forest'."

On the critics' point that the ISFR, bizarrely, not only report forest cover

for a new assessment year, but often go back and tweak forest cover values of previous years, the FSI said, "The experience gained over the years is helpful in better interpretation in successive cycles. The improved quality of data, better interpretation, extensive ground truthing and geographical area corrections resulted in revised estimates of previous cycles. Thus whenever, it is felt that we have better data for the previous cycle, the estimates are revised in order to give a true picture of real change."

There are many experts who, in fact, supported FSI's scientific method of assessment and questioned the critics, saying most of the points raised by them are "rooted in a lack of understanding of the difference between forest cover and tree cover on one hand and, and on the other hand, the need for retrospective corrections in assessments necessitated by advances in remote sensing technology that have brought in increased accuracy in assessments".

"Tea estates have been reported under tree cover (and not forest cover) because most tea plantations have shade trees raised to manage sunshine on the tea bushes. Wherever these shade trees provide more than 10% cover these are included in the tree cover," said forestry expert and retired Indian Forest Service (IFS) officer Promode Kant.

"Coffee and tea, coconut, and farm forestry plantations also provide ecological services much better than barren land in addition to providing livelihood systems to local people. Nowhere in the report, they have been equated with natural forests," said Bala Prasad, another retired IFS officer and former additional secretary, Panchayati Raj. <https://timesofindia.indiatimes.com>

China releases new moon map, most detailed to date

China has released a new comprehensive geologic map of the moon to a scale of 1:2,500,000, the most detailed to date. Chinese scientists from multiple research institutes and universities have created the high resolution topographic map based on data from China's lunar exploration Chang'e project and other data and research findings from international organizations.

The map includes 12,341 impact craters, 81 impact basins, 17 rock types and 14 types of structures, providing abundant information about geology of the moon and its evolution. It is expected to make a great contribution to scientific research, exploration and landing site selection on the moon. The Institute of Geochemistry of Chinese Academy of Sciences has led the project, along with other organizations such as Chinese Academy of Geological Science, China University of Geosciences and Shandong University. Previously, USGS Astrogeology Science Center completed and released a moon map to a scale of 1:5,000,000 in 2020. <https://news.cgtn.com>

RailTel and Esri India sign MoU

RailTel Corporation of India Ltd., Ministry of Railways and Esri India have signed an MoU to provide Cloud-based GIS Solutions to their users in the 'Government Sector'. This collaboration will address the strong emerging demand for 'GIS on Cloud'. With this partnership, 'Indo ArcGIS on Cloud' would now be available on RailTel Cloud, giving customers the much-needed advantage of scalability, agility and cost-efficiency. www.railtelindia.com

Open maps for Europe releases open cadastral map prototype

Open Maps for Europe has released an Open Cadastral Map prototype, which provides large-scale coverage for four countries. The data is now available via the Open Maps interface and this

first iteration includes Poland, The Netherlands, Czech Republic and Spain. The map takes INSPIRE open data and allows the user to find out what is available from national sources in one place before obtaining the data from the official provider. The cadastral map comprises four data types: Administrative Units, Cadastral Parcels (and Cadastral Zones), Buildings (and Building Parts) and Addresses. <https://eurogeographics.org>

Cadcorp launches new hosted Data Service

Cadcorp has updated its cloud services offering to include a new Data Service. The managed service provides direct access to a wide range of open data directly from a secure Cadcorp datastore. The service will allow customers to easily access data overlays within Cadcorp SIS Desktop and Cadcorp SIS WebMap. www.cadcorp.com

Doors open on world-leading European Glider Service Centre

The National Oceanography Centre (NOC) has partnered with Teledyne Marine, to open a new European Glider Service Centre. It will expand glider usage for both science and industry and provide scientific support and repair facilities for Teledyne Slocum Gliders. <https://noc.ac.uk>

New Disaster and Disruption Management System

AiDash has announced its Disaster and Disruption Management System (DDMS). DDMS is a satellite- and AI-powered SaaS offering that helps utility and energy companies as well as governments and cities, manage the impact of natural disasters, including storms and wildfires. The new system works in near real-time before, during, and after a major natural disaster or extreme weather event. The AI-powered system fuses satellite imagery, real-time weather data, span-level vegetation data, and historic outage and resource usage data for insights before, during, and after a major weather event. www.aidash.com

Chinese-made BeiDou satellite system output value hits new record

The output value of China's BeiDou Navigation Satellite System (BDS) reached a new high of 469 billion yuan (\$69 billion) in 2021, up 16.29 percent year on year, according to a white paper recently released.

The white paper, issued by the Global Navigation Satellite System (GNSS) and Location Based Service (LBS) Association of China, together known as GLAC, attributed the rapid growth to the global service of BDS-3 system started on July 31, 2020, which further stimulated demand for and attracted more investments in BDS technological applications. It further said that China remained the top source of international satellite navigation patent applications last year, totaling 98,000.

By the end of 2021, over 380,000 sets of BeiDou positioning, timing and short message communication terminals had been installed, and more than 7.9 million vehicles had been equipped with the BDS. Nearly 8,000 sets of BeiDou terminals of various types had been applied in the railway sector and over 100,000 agricultural machines had been equipped with the BeiDou self-driving system to monitor the harvest of staple crops and the operation of tractors around the clock. <https://news.cgtn.com>

Juniper Systems launches next-gen Geode GNS3 GNSS receiver

Juniper Systems has introduced the Geode GNS3 GNSS receiver, which allows users to collect real-time GNSS data with sub-meter, sub-foot and decimeter accuracy options.

Available in both single-frequency and upgradable multi-frequency antenna configurations, users have the level of accuracy needed to get the job done. www.junipersys.com

Enhanced operations in Australia by Satellogic

Satellogic Inc has announced that it is enhancing its operations in the Australian market to strengthen its regional customer relationships and provide local support for a growing APAC space economy. It currently operates 22 high-resolution satellites and expects to grow its constellation to 34 satellites by Q1 2023. By 2025, the Company expects to have over 200 satellites in orbit to provide daily remaps of the entire surface of the Earth, and up to 40 revisits of points of interest per day. www.satellogic.com

Freeform printing of satellite antennas in outer Space

Mitsubishi Electric Corporation announced that the company has developed an on-orbit additive-manufacturing technology that uses photosensitive resin and solar ultraviolet light for the 3D printing of satellite antennas in the vacuum of outer space.

The novel technology makes use of a newly developed liquid resin that was custom formulated for stability in vacuum. The resin enables structures to be fabricated in space using a low-power process that utilizes the sun's ultraviolet rays for photopolymerization. The technology specifically addresses the challenge of equipping small, inexpensive spacecraft buses with large structures, such as high-gain antenna reflectors, and enables on-orbit fabrication of structures that greatly exceed the dimensions of launch vehicle fairings. Resin-based on-orbit manufacturing is expected to enable spacecraft structures to be made thinner and lighter than conventional designs, which must survive the stresses of launch and orbital insertion, thereby reducing both total satellite weight and launch costs. www.mitsubishielectric.com

Unique Integration of UltraCam Eagle and LiDAR Scanner by 95West

95West Aerial Mapping offers innovative data collection by integrating an UltraCam Eagle Mark 3 aerial camera system with a Riegl VQ-1560 II-S airborne laser scanner in one aircraft. Simultaneous operations controlled with TopoFlight Systems management software cut flight time in half compared to separate missions, and the four-band large-format imagery and LiDAR point cloud are perfectly in sync. In early 2021, 95West purchased the new camera and LiDAR hardware, as well as a Cessna 208B Grand Caravan. Custom modifications were made to allow two camera ports to be added, and the combined system was ready to fly by September. The upgraded equipment allows the firm to tailor its products to the needs of the client and deliver custom solutions whenever necessary. www.vexcel-imaging.com

Aerial photography to update digital maps of Qatar completed

The Center for Geographic Information Systems (CGIS) of the Ministry of Municipality has completed the mission of aerial photography for all parts of Qatar and Halul Island to produce the 20cm-accuracy-rated aerial photographs and then update the digital linear maps of the country, as part of the implementation stages of the country's aerial surveys project.

The aerial photography, which lasted more than 20 days, contributes to providing all state institutions with aerial photographs and updated digital maps for use within the activities and projects of the FIFA World Cup Qatar 2022 tournament and in all other projects of the State in various fields. In the work of aerial surveys and remote sensing, the CGIS used manned aircraft to achieve integration with other data sources that the center currently uses, such as satellite images, mobile field surveys, and drones.

As part of the plan to develop national standards and specifications related to geographic information systems at the state level, carrying out aerial surveys and remote sensing using piloted aircraft comes in integration with other data sources currently used to process and extract rectified aerial images, tilted aerial images, linear data, 3D model data and altitude model, digital (DEM), remote sensing, LIDAR data, bathymetric survey data for bathymetry, marine survey and hyperspectral imaging. www.gulf-times.com

Remote sensing research improves hurricane response

Researchers with the FAMU-FSU College of Engineering's Resilient Infrastructure and Disaster Response (RIDER) Center are investigating better ways to predict where road-clogging debris will be most severe after tropical cyclones..

Researchers used satellite images to measure the amount of vegetation in Bay County, Florida, before and after two tropical storms and three hurricanes, including Hurricane Michael, a Category 5 storm that devastated the county in 2018. That gave them an estimate of how much vegetative debris those storms caused and where debris was heaviest. They were able to correlate debris measurements with factors such as wind speed, initial amount of vegetation and roadway density.

The researchers found debris was heavier in suburban and urban areas, which have a high density of people and roads, compared with rural areas. Although vegetation is not the only type of debris caused by a hurricane, it is an important predictor of where roads will be blocked.

Researchers aim to develop a tool that gives emergency management planners an estimate of the debris storms are likely to generate – allowing officials to plan, for example, where to position trucks and collection zones ahead of storms. <https://news.fsu.edu>

Hitachi launches Lumada Inspection Insights

Hitachi, Ltd. has launched Lumada Inspection Insights, its end-to-end portfolio of digital solutions for the inspection, monitoring, and optimization of critical assets. It enables customers to automate asset inspection, support sustainability goals, improve physical security, and reduce risks and impacts related to storms or fires by using powerful artificial intelligence (AI) to analyze photographs and video, including LiDAR, thermal and satellite imagery. The new portfolio addresses various root causes of failures and forced shutdowns by deploying AI and machine learning (ML) to analyze a wide spectrum of image types, assets and risks. Predictive analytics assesses the risks to operations or environment, and organizations can streamline remediation before outages occur. www.hitachi.com

Demonstration of optical inter-satellite links in low earth orbit

CACI International has successfully demonstrated space to space optical communications links in low earth orbit (LEO) in partnership with the Defense Advanced Research Projects Agency (DARPA) and the Space Development Agency (SDA) as part of the Mandrake II program.

Mandrake II is a joint risk-reduction program with DARPA, SDA and the Air Force Research Laboratory's Space Vehicles Directorate (AFRL/RV) to evaluate the pointing, acquisition, and tracking algorithms that allow for optical communication terminals to establish and maintain high-speed communication links in the upcoming Blackjack and SDA Transport and Tracking Layer constellations. This successful test, completed using CACI's CrossBeam free-space optical terminals, is the first step in establishing more secure, space-based communications networks for defense agencies using more powerful, efficient technology that can transmit more data, faster. caci.com

EcoStruxure for eMobility in buildings

Schneider Electric has launched a new EV charging solution for efficient, resilient, and sustainable electric mobility and net-zero buildings. EcoStruxure for eMobility provides more than just EV chargers, it is an end-to-end connected solution that is easy to install, maintains building power reliability, and provides a convenient experience for EV drivers. www.se.com

5G innovation lab by Tech Mahindra

Tech Mahindra has inaugurated a 5G Lab in Bellevue, WA that will curate vertical solutions in the telco space to help customers achieve their future business ambitions through 5G and related technology. The lab will combine an ecosystem of partners (both telecom and cloud) and help build end-to-end solutions for enterprises. The innovation lab will witness software and hardware developers, operators, and cloud service providers coming together to co-create solutions that will define a new era of customer experience powered by 5G. www.techmahindra.com

Buildings IoT launches UK operations

To decarbonize buildings and help advance Net-Zero initiatives, US-based Buildings IOT has launched operations in the UK to serve the unique needs of building stakeholders in Europe. The Buildings IOT UK team will be seeking opportunities in several London-based commercial buildings, including office and manufacturing, to improve the occupant experience as well as realize overall operational efficiencies. www.BuildingsIOT.com

Hesai reached strategic cooperation with WeRide

Hesai Technology and WeRide announced a new strategic cooperation agreement. Both the parties will promote the autonomous vehicle

application of automotive grade, hybrid solid-state lidar, empowering scale deployment and commercial application of WeRide's autonomous driving technology. www.weride.ai

Deep learning for autonomous vehicles with Microsoft

Wayve announced that it is working with Microsoft to leverage the supercomputing infrastructure needed to support the development of AI-based models for autonomous vehicles (AVs) on a global scale. This announcement follows Microsoft's participation in Wayve's \$200M Series B investment round.

The companies are bringing together Wayve's expertise using deep neural networks and vast quantities of data to train AI models with Microsoft's engineering excellence in powering large-scale AI systems. Together, they aim to unlock the power of deep learning systems for autonomy, which holds the promise of being able to scale faster to new places than rules-based approaches.

Traditional self-driving systems rely on expensive hardware, HD mapping, and complex localization systems that can take months and years to re-engineer for any new location. <https://wayve.ai>

Extra large autonomous undersea vehicles

Anduril Industries and the Australian Defence Force are entering into commercial negotiations for a US\$100m co-funded design, development and manufacturing program for Extra Large Autonomous Undersea Vehicles (XL-AUVs) for the Royal Australian Navy. The XL-AUV is a modular, customizable and can be optimized with a variety of payloads for a wide range of military and non-military missions such as advanced intelligence, infrastructure inspection, surveillance, reconnaissance and targeting. www.anduril.com

Drone Festival – Bharat Drone Mahotsav 2022

Prime Minister Shri Narendra Modi inaugurated Drone Festival - Bharat Drone Mahotsav 2022 on May 27, 2022. He also interacted with Kisan drone pilots, witnessed open-air drone demonstrations and interacted with startups in the drone exhibition centre. Several union ministers, leaders and entrepreneurs of drone industry were among those present on the occasion.

Addressing the gathering, the Prime Minister conveyed his fascination and interest in the drone sector. He cited PM Swamitva Yojana as an example of how drone technology is becoming the basis of a major revolution. Under this scheme, for the first time, every property in the villages of the country is being digitally mapped and digital property cards are being given to the people.

Highlighting the importance of drone technology in the fields of defence, disaster management, agriculture, tourism, film and entertainment, he said that the use of this technology is bound to increase in the coming days. He also narrated the use of drones in his official decision making through examples of PRAGATI reviews and Kedarnath projects.

Drone technology is going to play a major role in empowering farmers and modernize their lives. He also talked about continued dependence on the revenue department with regard to activities ranging from land records to flood and drought relief. The drone has emerged as an effective tool to tackle all these issues. pib.gov.in

DroneAcharya Aerial Innovations secures USD 4.6 Million investment

Closing their pre- seed round at \$4.6 Million (INR 35.7 Cr.), Pune – based drone startup, DroneAcharya Aerial Innovations is the only Indian startup till date to have raised this amount. It is a drone service provider, manufacturer, and DGCA – approved remote pilot training organization. The Indian government has aided the growth of the drone industry in India by enacting supportive regulations and providing subsidies. <https://droneacharya.com>

Continental Drones and Wingcopter to transform African supply chains

German drone delivery pioneer Wingcopter and Continental Drones Ltd., a subsidiary of Ghana- and Dubai-based Atlantic Trust Holding, have signed a partnership agreement to help establish drone-based delivery networks across the African continent. These networks will dramatically improve the reliability and efficiency of existing supply chains but also help create completely new ones. In many African regions, insufficient infrastructure is one of the biggest barriers to universal health coverage and economic development. Setting up large-scale drone delivery networks across African airspace will propel logistics in these countries to a new level and help build an entirely new transport framework – much faster, cheaper, more sustainable, and more efficient than the development of conventional ground-based infrastructure with all its unhealthy and climate-damaging emissions. <https://wingcopter.com>

Skyline Nav AI, Draper win contract

The project is led by Skyline Nav AI, which has secured a contract from the U.S. Air Force Research Laboratory (AFRL) to provide GPS-independent localization capability for the ATAK platform. Draper will integrate Skyline’s application into ATAK’s front-end. It is currently on contract with the U.S. Department of Defense and several government agencies to provide ongoing development, training and support for multiple TAK platforms. www.skylinenav.com

BIRD Aerosystems launches a new business line of Land systems

BIRD Aerosystems launches its new business line of Land systems and unveils two new products for the first time at the Eurosatory exhibition: Hybrid-Eye, an advanced hybrid detection system that enhances the protection of armored vehicles, and μMPR, a miniature airborne radar for ground and maritime border surveillance. The new all-in-one miniaturized solutions are ideal for medium to small platforms, offering a new level of detection and protection that wasn’t part of the capabilities of such systems before. www.birdaero.com

Honeywell strengthens industrial navigation portfolio

Honeywell recently introduced three new navigation systems: the HGuide o360 inertial/global navigation system (INS/GNSS) navigator, the HGuide n500 inertial navigator and the HGuide g080 GNSS receiver. The systems are designed for various industrial applications across air, land and sea vehicles and related equipment, where positioning and attitude information is required in real time. All deliver accurate navigation even in GPS denied environments. <https://aerospace.honeywell.com>

High-accuracy OEM GNSS receiver module by Trimble

Trimble BD9250 is a dual-frequency OEM GNSS receiver module that supports



“The monthly magazine on Positioning, Navigation and Beyond”

Download your copy of Coordinates at

www.mycoordinates.org

Trimble RTX correction services. The receiver is designed to deliver high-accuracy positioning for a range of high volume, autonomous-ready applications. It is a compact receiver with an industry-standard form factor and pinout, allowing for easy system integration and configuration. Equipped with Trimble's advanced ProPoint™ positioning engine, the BD9250 is compatible with Trimble RTX correction services or RTK and supports all major GNSS constellations. www.trimble.com

Tersus GNSS releases white paper on ExtremeRTK Technology

Tersus GNSS has released a white paper on ExtremeRTK Technology. It demonstrates how ExtremeRTK Technology delivers excellent performance in all manner of surveying scenarios and describes its impressive compensated results when performing tilt surveys — even tilt at angles greater than 90°.

According to the paper, “ExtremeRTK integrates the receiver’s hardware, high-precision baseband IC [integrated circuit], RTK engine, GNSS/INS coupling algorithm, etc. It enables unprecedented performance stability in challenging environments and prevents occurrences of occasional RTK positioning outliers.” www.tersus-gnss.com

Mayflower receives FAA TSO-C190 authorization

Mayflower Communications Company, Inc. has received technical standard order (TSO-C190) authorization from the US Federal Aviation Administration (FAA) for both models of its MAGNA GPS Anti-Jam product. The products are the first and only GPS Anti-Jam systems in the industry to receive the FAA TSO Authorization for installation on both military and civilian aircraft.

The MAGNA Anti-Jam products are comprised of two different models, the MAGNA-Federated (MAGNA-F) and the MAGNA-Integrated (MAGNA-I).

Mayflower’s MAGNA products build on Mayflower’s highly SWaP-optimized GPS Anti-Jam (AJ) antenna technologies, such as Small Antenna System (SAS). mayflowercom.com

Collision risk analysis and avoidance maneuver calculation software

Following an open European tender, GMV has been awarded a new contract by the Centre for the Development of Industrial Technology (CDTI) to develop software for advanced collision risk analysis and avoidance maneuver calculation for European satellite operators subscribed to the EU SST system’s collision avoidance service.

The new software, called CONAN (CONjunction ANALysis Software), will have a dual purpose: first, to increase the capabilities and improve the response times of the S3TOC (Spanish Space Surveillance and Tracking Operations Centre) and secondly, to provide European satellite operators subscribed to the EU SST system’s collision avoidance service with their own conjunction analysis capability, as it will also be deployed in their control centers. www.gmv.com

Septentrio expands its product portfolio for marine market

Septentrio has announced the launch of two new GNSS products for marine applications: AsteRx-U3 Marine and AsteRx-m3 Fg. Both products offer accurate positioning near and offshore via centimeter-level RTK or the built-in Fugro PPP sub-decimeter subscription service, delivered either over NTRIP internet or over L-band satellite. septentrio.com

GNOMES-3 GNSS radio-occultation satellite launched

A new GNSS radio-occultation (RO) satellite is now in orbit. The GNOMES-3 — GNSS Navigation and Occultation Measurement Satellite — flew aboard the SpaceX Falcon 9 Transporter-4 rideshare mission on

April 1 and was launched into a 646-km circular sun-synchronous orbit. The payload was powered on and operating nominally within four days of launch.

The GNOMES-3 was manufactured for PlanetiQ by Blue Canyon Technologies LLC, a wholly owned subsidiary of Raytheon Technologies. It joins GNOME-2 on orbit and is expected to achieve highly accurate GNSS-RO measurements using the fourth-generation Pyxis-RO sensor. PlanetiQ plans to launch more Pyxis-RO atmospheric and ionospheric sounding spacecraft in 2023. In all, PlanetiQ plans for a fleet of 20 GNOMES by 2024. <http://planetiq.com>

Xona's private GNSS satellite passes pre-launch testing

Xona Space Systems announced that their first in-space demonstrator has been delivered to Spaceflight Inc. for final integration after successfully completing testing. Xona is an aerospace startup developing a precision navigation and timing system in low Earth orbit. It plans to build an independent high-performance satellite navigation and timing system to meet the needs of intelligent systems.

It is launching Huginn, the first of two missions, demonstrating the capability of its Pulsar constellation. Pulsar’s architecture uses small, powerful satellites in low Earth orbit, more than 20 times closer to Earth than GPS satellites, which are in medium Earth orbit. www.xonaspace.com

Advanced Navigation adds sensing capabilities with vai acquisition

AI robotics and navigation technology company Advanced Navigation has acquired Australian National University (ANU) spinout Vai Photonics. Vai is developing photonic sensors for precision navigation and joins Advanced Navigation to commercialize its research into autonomous and robotic applications across land, air, sea, and space. The technology has been in development for over 15 years at ANU. www.photonics.com

SUBSCRIPTION FORM

YES! I want my **Coordinates**

I would like to subscribe for (tick one)

1 year 2 years 3 years

12 issues 24 issues 36 issues
Rs.1800/US\$140 Rs.3400/US\$200 Rs.4900/US\$300

* 

First name

Last name

Designation

Organization

Address

.....

City Pincode

State Country

Phone

Fax

Email

I enclose cheque no.

drawn on

date towards subscription

charges for Coordinates magazine

in favour of 'Coordinates Media Pvt. Ltd.'

Sign Date

Mail this form with payment to:

Coordinates

A 002, Mansara Apartments
C 9, Vasundhara Enclave
Delhi 110 096, India.

If you'd like an invoice before sending your payment, you may either send us this completed subscription form or send us a request for an invoice at iwant@mycoordinates.org

* Postage and handling charges extra.

MARK YOUR CALENDAR

July 2022

Esri User Conference
11-15, July 2022
San Diego, CA, USA
www.esri.com

IGARSS 2022 (hybrid form)
17-22 July 2022
Kuala Lumpur, Malaysia
<https://igarss2022.org>

August 2022

GeoCart'2022
24 - 26 Aug
Wellington, New Zealand
www.cartography.org.nz

September 2022

International Symposium of Commission
4: Positioning and Applications
5 to 8 September 2022
www.iag-commission4-symposium2022.net

15th Conference on Spatial
Information Theory (COSIT)
5-9 Sep 2022
Kobe, Japan
cosit2022.iniad.org

Commercial UAV Expo Americas
6-8 September 2022
Las Vegas, USA
www.expouav.com

17th Symposium on Location
Based Services (LBS2022)
12-14 Sep 2022
Munich, Germany
lbsconference.org

18th International Conference on
Geoinformation and Cartography
14-16 Sep 2022
Zagreb, Croatia
www.kartografija.hr

EuroCarto 2022
19-21 Sep
Vienna, Austria
www.eurocarto2022.org

ION GNSS+ 2022
19-23 September
Denver, CO, USA
www.ion.org/gnss/index.cfm

October 2022

Intergeo Hybrid
18-20 October 2022
Essen, Germany
www.intergeo.de

November 2022

Trimble Dimensions+
7-9 November 2022
Las Vegas, USA
<https://dimensions.trimble.com>

Belgian church spire scanned by a Riegl scanner

The Sint-Jan-De Doperkerk Church in Belgium recently retained LSBbvba to perform a 3D scan on the inside and outside of its historic chapel spire. The aim of this project is to capture data necessary for a renovation of the tower spire. Detailed façade plans and heights within the tower were needed regarding the stairs and bell levels, especially since parts of the spire were rotted and not safe for contractors to step through for observation.

A RIEGL VZ-400i Terrestrial Laser Scanner fitted to a tilt mount at a 45-degree angle was able to document the needed data, which was processed through RiSCAN PRO – everything being done completely from cloud to cloud.

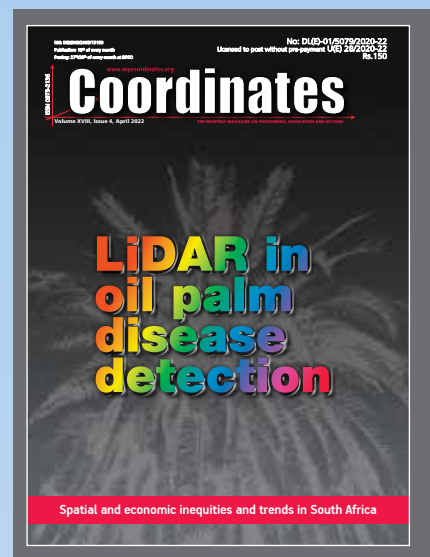
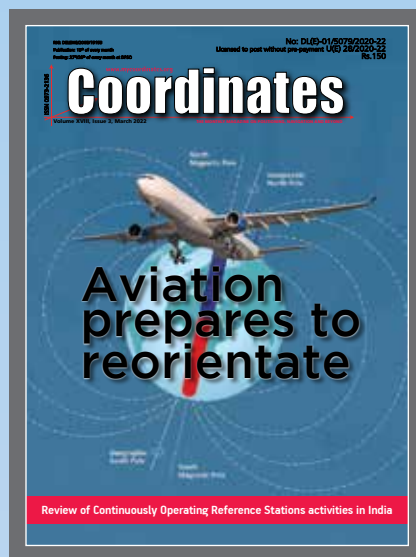
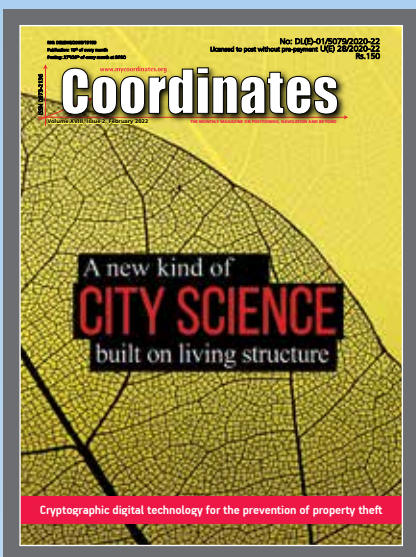
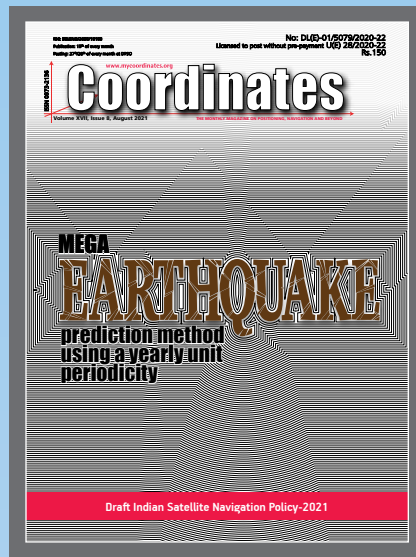
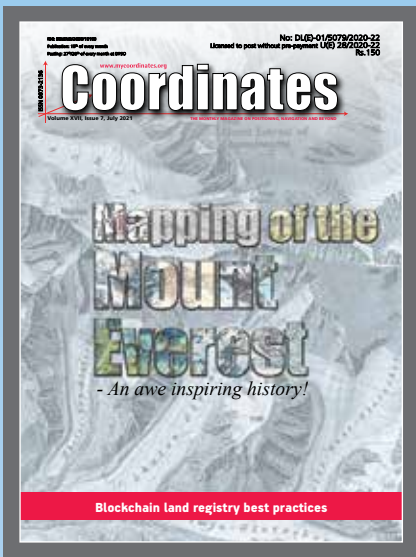
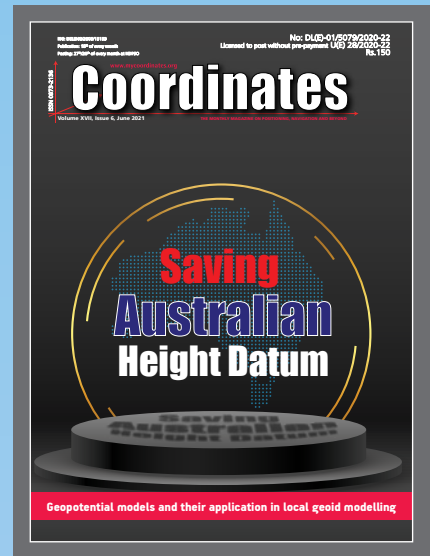
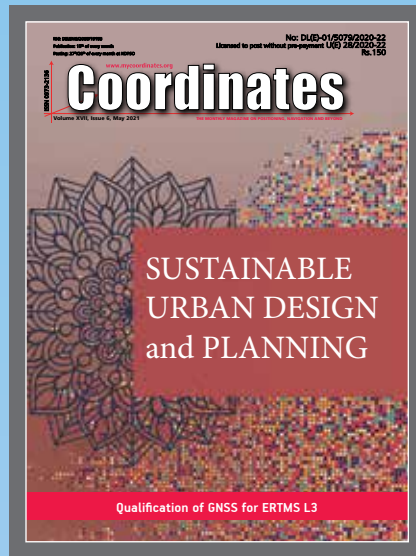
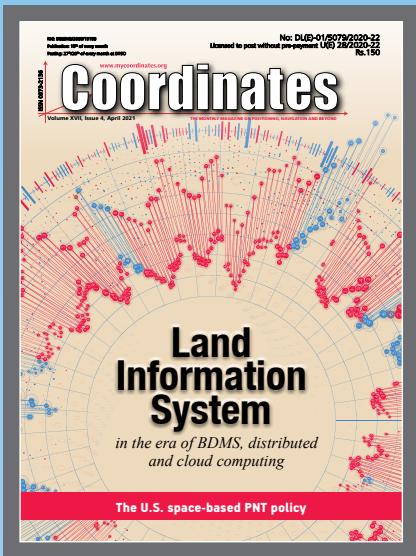
IDS GeoRadar launches Ai.DA

IDS GeoRadar has announced the new solution for geotechnical professionals that pioneers the introduction of Artificial Intelligence in slope stability monitoring - Ai.DA, the AI-based software monitoring tool for Guardian.

Ai.DA is an Artificial Intelligence based software tool providing an additional smart processing layer to radar data. Through the use of AI algorithms, it simplifies the identification of movements from possible residual noise by evaluating the consistency of the detected movement trend with typical slope instabilities behaviors and models, helping professionals to optimize processes and take better decisions. <https://idsgeoradar.com>

Location data expertise for food tech companies

Transerve announced its support for location data expertise to food tech companies as food tech-companies like Zomato, Swiggy, and Blinkit create a buzz with their 10-minute delivery plan. Acing the high-tech marvel, food delivery market is expected to grow USD 15 billion by 2023. 



“The monthly magazine on Positioning, Navigation and Beyond”
Download your copy of Coordinates at www.mycoordinates.org



Test Space Qualified Receivers for When the Sky Is Not Your Limit

LabSat GNSS simulators offer multi-constellation and multi-frequency capabilities for **reliable, repeatable and consistent testing.**



Space Scenarios

Create **custom scenarios** to test launch, in-orbit and re-entry trajectories



True Horizon

Follow the **True Horizon** with a dynamically changing elevation mask



Real-Time Option

Generate **real-time GNSS** RF signals with a current time stamp



Easy to Use

One touch **Record & Replay** with simple configuration

RECORD / REPLAY / SIMULATE

labsat.co.uk/space